



ALMA MATER STUDIORUM
UNIVERSITÀ DI BOLOGNA

ARCHIVIO ISTITUZIONALE
DELLA RICERCA

Alma Mater Studiorum Università di Bologna Archivio istituzionale della ricerca

Forecasting electricity prices with expert, linear, and nonlinear models

This is the final peer-reviewed author's accepted manuscript (postprint) of the following publication:

Published Version:

Anna Gloria Billé, Angelica Gianfreda, Filippo Del Grosso, Francesco Ravazzolo (2023). Forecasting electricity prices with expert, linear, and nonlinear models. INTERNATIONAL JOURNAL OF FORECASTING, 39(2 (April-June)), 570-586 [10.1016/j.ijforecast.2022.01.003].

Availability:

This version is available at: <https://hdl.handle.net/11585/897303> since: 2024-03-11

Published:

DOI: <http://doi.org/10.1016/j.ijforecast.2022.01.003>

Terms of use:

Some rights reserved. The terms and conditions for the reuse of this version of the manuscript are specified in the publishing policy. For all terms of use and more information see the publisher's website.

This item was downloaded from IRIS Università di Bologna (<https://cris.unibo.it/>).
When citing, please refer to the published version.

(Article begins on next page)

Forecasting Electricity Prices with Expert, Linear and Non-Linear Models

Anna Gloria Billé^a, Angelica Gianfreda^{c,d}, Filippo Del Grosso^b, Francesco Ravazzolo^{b,e,f}

^a*Department of Statistical Sciences, University of Padua, Italy*

^b*Faculty of Economics and Management, Free University of Bozen–Bolzano, Italy*

^c*Department of Economics, University of Modena and Reggio Emilia, Italy*

^d*Energy Markets Group, London Business School, London, UK*

^e*BI Norwegian Business School, Norway*

^f*RCEA, Rimini Center for Economic Analysis, Italy*

Abstract

This paper compares several models for forecasting regional hourly day-ahead electricity prices, while accounting for fundamental drivers. Forecasts of demand, in-feed from renewable energy sources (RES), fossil fuel prices, and physical flows are all included in linear and nonlinear specifications, ranging in the class of ARFIMA–GARCH models; hence including parsimonious autoregressive specifications (known as *expert-type* models). Results support the adoption of a simple structure that is able to adapt to market conditions. Indeed, we include forecasted demand, wind and solar power, actual generation from hydro, biomass and waste, weighted imports and traditional fossil fuels. The inclusion of these exogenous regressors, in both the conditional mean and variance equations, outperforms in point and, especially, in density forecasting when the Superior Set of Models is considered. Indeed, using the Model Confidence Set and considering the northern Italian prices, predictions indicate a strong predictive power of regressors, in particular in an expert model augmented for GARCH-type time-varying volatility. Finally, we find that using professional and more timely predictions of consumption and RES improves the forecast accuracy of electricity prices more than predictions publicly available to researchers.

Keywords: Demand, Wind, Solar, Biomass, Waste, Fossil Fuels (coal, natural gas, CO₂),

Weighted Inflows, Commercial and Public Forecasts

JEL Classification: C13, C22, C53, Q47

14 **1. Introduction**

15 Forecasting day-ahead electricity prices has always attracted the attention of practitioners and
16 scholars because trading decisions are based on strategic and stochastic components, like arbitrage
17 speculations, impossibility to store electricity and variability introduced into the system by effects
18 of new regulations and imperfect predictability of fundamental drivers. This paper investigates
19 both aspects.

20 Day-ahead electricity prices are determined for each hour of the following day, by the
21 intersection of the aggregated curves of demand and supply. Therefore, factors that influence
22 both curves have been largely investigated in price modelling. Fundamental variables as forecasted
23 demand and weather conditions have been taken into account for the demand curve, whereas the
24 predicted intermittent generation by renewable energy sources (RES) has been recently considered
25 a risk source in the supply curve, together with import and export flows and the international
26 movements of fossil fuel prices used in traditional thermal plants; for extensive reviews see Weron
27 (2014), Nowotarski and Weron (2018) and Hong et al. (2020).

28 All these variables must be considered in the formulation of ex-ante expectations of day-
29 ahead electricity prices. Furthermore, in recent years, the power generated by RES has increased
30 substantially due to incentives and the worldwide goal of reducing carbon emissions. Indeed, as
31 a country in the European Union (EU), Italy is among the top six countries in the world for
32 renewable power capacity (not including hydro), after Germany and together with the United
33 Kingdom. Specifically, Italy is among the top EU countries for wind and solar photovoltaic (PV)
34 capacity additions in 2017 (REN21, 2018).

35 The increasing RES generation dispatched on the day-ahead (and intra-day) market has a
36 twofold effect. According to the merit order, producing units that pollute less have the priority
37 of dispatch and move the supply curve towards the right as soon as their generation increases.
38 Consequently, equilibrium prices decrease due to the new RES generation. On one hand, all this
39 has the effect of moving thermal conventional technologies out of the day-ahead market, and,
40 on the other hand, it reduces the spreads between maximum and minimum prices which make
41 water pumping units less profitable. They have no more time-arbitrage opportunities in buying
42 electricity in off-peak hours and selling it during peak hours in the day-ahead market. Then, those
43 units allowed to act in real-time sessions can try to recover there their profits. This occurred in

44 Italy attracting the attention of the energy regulator in 2016, when enormous costs were generated
45 within the system as a consequence of the speculative trading of few thermal units. Gianfreda et al.
46 (2018) studied the auction/bid data for the the northern Italian zone, characterized by a high solar
47 PV and hydro penetration. Considering all market sessions, from the day-ahead to real time and
48 passing through intra-day sessions, they provide empirical evidence that balancing costs increased
49 between two samples associated with low (in years 2006–08) and high (in years 2013–15) RES levels.
50 They studied the up- and down-regulation in the balancing market sessions, which differ across the
51 Italian physical zones because of the location and characteristics of RES capacity. It is intuitive that
52 a geographically balanced portfolio may compensate easily and promptly any variations in demand
53 or in generation (due to the forecast errors of RES output). However, the authors observed that
54 the northern zone appears to be subject to a systematic overestimation of PV generation capacity
55 sold in the day-ahead market, hence requiring up-regulation to restore the system equilibrium at
56 a price which is generally more costly than the one for down-regulation. Considering that the
57 seasonality of solar production reduces the residual demand covered by conventional technologies
58 during hours of irradiation and that it requires a strong increase in programmable and flexible
59 production at sunset, the evening ramp increased from 8250 MW in 2012 to 11,050 MW in 2014;
60 and it was contemporary paired with the dismissal of a number of old thermal units. They observe
61 that some generators, allowed to act on the balancing market, were withholding capacity on the
62 day-ahead market (or closing their net position to zero over day-ahead and intra-day sessions)
63 and selling energy in the real-time sessions, where the pay-as-bid pricing mechanism grants the
64 (higher) price declared in accepted bids. These Italian sessions have a limited number of traders
65 and are dominated by conventional (thermal, hydro and water pumping) technologies with no
66 competition from RES units (indeed they are not allowed to participate into the Italian balancing
67 sessions) and so they can only reduce the day-ahead prices, as an effect of the merit order.

68 To overcome these critical issues, some EU countries, including Italy, have started to discuss the
69 possibility of allowing RES units to act also in the balancing markets. However, in the meanwhile,
70 the prediction of prices on the day-ahead market is becoming an increasingly important and
71 essential step in the evaluation of trading strategies, since thermal conventional as well as water
72 pumping units consider the price spreads among the various sequential sessions; together with the
73 possibility to act over a long-term capacity market. Based on all these arguments and because
74 of the raised issue in 2016, Italy is an excellent case study. Moreover, the zonal structure allows

75 the consideration of the operators' bidding behaviour across different areas and according to the
76 composition of their generation mix. Northern Italy is, therefore, an exceptionally good example for
77 several reasons. First, the zone is well interconnected with foreign countries, from whom electricity
78 can be imported at lower prices. Second, a high share of solar PV generation has been observed
79 in recent years. Third, most of the hydro generation is located in the Alps. Fourth, and more
80 importantly, the demand of electricity in this zone represents almost half of the national demand;
81 hence, variations in demand and supply can boost the strategic use of balancing sessions. Finally,
82 all three thermal conventional, hydro and water pumping technologies act in this zone across
83 all different market sessions. Therefore, the prediction of day-ahead electricity prices observed
84 in Northern Italy can increase the understanding of the main drivers of these prices, and could
85 contribute to the monitoring (hence in controlling) the bidding strategies across market sessions,
86 according to the price levels expected in the day-ahead market. Other studies based on different
87 markets and considering bidding strategies and their associated economic value are presented in
88 Bunn et al. (2018), Lisi and Edoli (2018), Abramova and Bunn (2020) and Kath et al. (2020).

89 Others attempts to capture the impacts of economic, technical, strategic, and risk factors on
90 intra-day prices are presented in Karakatsani and Bunn (2008). Oberndorfer (2009) focused on
91 the relationship between energy market developments, external shocks, and pricing of European
92 utility stocks. Hickey et al. (2012) implemented ARMAX-GARCH models with trend, dummy
93 variables for seasonality and load for five MISO pricing hubs. Subsequently, Maciejowska and
94 Weron (2016) focused on the increased granularity of data available on the British market (where
95 prices have a half-hour frequency) to test a set of fundamental explanatory variables (i.e. natural
96 gas, coal, and CO₂ emissions). de Marcos et al. (2019) proposed an econometric and fundamental
97 approach to forecast short-term prices in the Iberian market by pairing a neural network with a set
98 of expected and actual fundamental variables. Gianfreda et al. (2020) compared several univariate
99 and multivariate models augmented with fundamental variables, including demand forecasts and
100 forecasted production from renewable energy sources, to predict hourly day-ahead electricity prices
101 in several European markets.

102 According to the literature, few papers have inspected the predictability of day-ahead prices in
103 Northern Italy. The most notable studies are Gianfreda and Grossi (2012), Shah and Lisi (2019)
104 and Bernardi and Lisi (2020). The latter two papers adopt a generalised additive location-scale
105 model with a non-parametric estimation of the conditional mean and variance and a nonparametric

106 functional autoregressive model based on individual bids. Whereas the former one considers
107 the Italian zonal prices during years 2006–2008, when RES had a limited (or none) role in the
108 determination of prices. Indeed, in that contribution, wind, solar, or hydro were not considered.

109 Accounting for the arguments that strong electricity price autocorrelations and long memory
110 may be induced by the mean–reverting nature of market fundamentals, or by the highly repetitive
111 nature of electricity auctions or also by the increased market integration (Knittel and Roberts, 2005;
112 Haldrup and Nielsen, 2006; Conejo et al., 2005; Koopman et al., 2007 and Jeon and Taylor, 2016),
113 we select AR(FI)MA–GARCH–type models and compare their forecasting ability with/without a
114 set of regressors, while adopting a rolling window approach and an adaptive scheme. The former
115 approach recalls the dynamic evolution of fundamentals over time, in line with the time–varying
116 parameter regression model implemented in Karakatsani and Bunn (2008) to adapt continuously
117 price structures to market changes. Furthermore, the latter scheme develops to the estimation
118 strategy implemented in Weron and Misiorek (2008), Chen and Bunn (2014) and Maciejowska
119 and Weron (2016), by extending the selection to both the autoregressive and moving average lag–
120 orders for each calibration window and each model specification, including the options to switch
121 from one model to another one and to replace negative forecasted prices with null prices (since that
122 negative pricing is not allowed in the Italian market). Additionally, parsimonious autoregressive
123 models extended for regressors and time-varying volatility have been included in the analysis;
124 following Ziel (2016) and Ziel and Weron (2018). Therefore, in what follows we refer to these
125 models as those built on some *experts’ knowledge*.

126 It is worth noting that we expand these models by including our set of fundamentals (that
127 is predicted values for wind, solar PV, and demand, together with actual values for biomass,
128 hydro, waste, and weighted flows plus fossil fuel prices). Then, we explore a total of 58 linear and
129 nonlinear specifications to provide empirical evidence of their forecasting performance, given the
130 mixed results in the literature (see Hong et al., 2014 among others). Specifically, we test several
131 AR(FI)MAX–GARCH and *expert-type* models, and we additionally investigate LASSO variants
132 for the selection of exogenous regressors, dummy variables, and autoregressive terms when the lag
133 ordering is set at high values. Recent literature on LASSO and its applications can be found in
134 Ziel et al. (2015), Ziel and Weron (2018), Uniejewski et al. (2019) and Messner and Pinson (2019);
135 among others.

136 In addition, our contribution relies on applying both the Diebold–Mariano (DM) (Diebold and

137 Mariano, 1995) and the Model Confidence Set (MCS) (Hansen et al., 2011) testing procedure to
138 account for the large model uncertainty in evaluation. A density forecast exercise is also provided
139 to guide practitioners in choosing the best model according to different hours.

140 More importantly, given the issue of data availability, market transparency and economic
141 relevance of accurate predictions as discussed in Kezunovic et al. (2020) and Gonçalves et al.
142 (2021), we include an interesting analysis in which we compare the forecasting performance when
143 professional and more timely forecasts are used in place of public and freely available forecasts.
144 Maciejowska et al. (2021) show that these freely available forecasts of fundamental variables are
145 biased and could be improved. We confirm that including fundamental factors improves the
146 forecasting ability. In particular, our expert EX₄X model augmented with fundamental drivers
147 gives more accurate point forecasts: none of the other 57 models is statistically superior to it at
148 any hour, despite the large number of specifications found in the model confidence set.

149 The evidence is different when the loss function is generalized to the density forecasting: all
150 models with GARCH time-varying volatility give the most accurate density forecasts and they are
151 statistically superior to models that exclude it.

152 When professional forecasts are used, the forecast power further increases, in particular for the
153 early-morning and peak hours.

154 In details, we find that the inclusion of exogenous regressors reduces both the RMSEs and
155 the CRPSs, especially during peak hours. More specifically, an expert model (our EX₄X) and its
156 GARCH specifications drastically outperform all other models in point forecasts. From a practical
157 point of view, this expert model and its GARCH variants are the only ones retained for all hours
158 in the MCS, and especially when hour 19 is considered. In addition, the results on CRPS and
159 DM show that there are substantial improvements when all models are enlarged to include the
160 GARCH time-varying volatility.

161 In a context characterized by a limited number of regressors with respect to the amount of
162 statistical information available, we find that there are no substantial improvements when LASSO
163 models are considered.

164 In addition, for the first time to our best knowledge, we provide the empirical evidence that
165 using commercial forecasts improves substantially price forecasts, especially during hours 1-7 and
166 peak hours 8-20. Then, as soon as the forecasting horizon increases, as after hour 21, the benefits
167 of these more timely forecasts disappear. And we emphasize that this evidence is driven by the

168 usage of professional forecasts and not by considering simple or complex models (in both cases, we
169 observe improvements).

170 Finally, we also assess the coefficients of the exogenous regressors in our best model to
171 investigate their degree of significance through the considered sample. We provide evidence that a
172 model accounting for the dependence of prices over their demeaned prices of the previous 8 days,
173 and including forecasted load, wind and solar, as well as actual hydro and natural gas prices, seems
174 'expert' enough to explain well and forecast even better the northern Italian day-ahead prices.

175 The remainder of the paper is structured as follows. Section 2 presents a brief description of the
176 Italian market with a focus on the northern zone. Section 3 provides a detailed description of the
177 data employed and the methodological strategy used to predict hourly electricity prices. Section
178 3.3 describes the estimation and Section 4 presents the results. Finally, Section 5 concludes.

179 **2. The Italian Market Structure and the Northern Zone**

180 The Italian electricity market is structured into three main segments: the day-ahead, the
181 intraday, and the ancillary services markets. The latter is paired by the balancing market operated
182 in real time on the day of delivery. Day-ahead and intraday segments are open to a variety of
183 national and international operators (producers, consumers, traders), for a total of 258 different
184 market participants in 2017.¹ Market participation is voluntary both in the day-ahead and in
185 the intraday markets, whereas it is compulsory in the ancillary services market sessions where
186 only balancing units with the required degree of flexibility are allowed to act. We focus on the
187 day-ahead market, which opens nine days before the day of delivery and closes at noon on the day
188 before delivery.

189 The Italian electricity market is structured into geographical and foreign virtual zones. The
190 geographical zones represent a portion of the national grid delimited by bottlenecks in transmission
191 capacity, and these are Northern Italy, Central-Northern Italy, Central-Southern Italy, Southern
192 Italy, Sicily, and Sardinia. The foreign virtual zones are points of interconnection with neighbouring
193 countries. In this paper we consider Northern Italy; thus, the foreign virtual zones in this analysis

¹The spot market is complemented by the forward market (a platform for different types of contracts) and by the bilateral contract platform (where all OTC energy transactions that require flows through the power grid are registered).

194 are France, Switzerland, Austria, and Slovenia.

195 Each geographical and virtual zone yields an hourly (clearing) price, obtained from an implicit
196 bidding mechanism in which pairs of quantities (in MWh) and prices (in €/MWh) are considered
197 by accounting for the market splitting in case of congestions. Therefore, in the same hour, zonal
198 prices in contiguous market zones can differ depending on transmission bottlenecks. The zonal
199 prices concur to generate the single national price (or *prezzo unico nazionale*, PUN), that is the
200 average of zonal day-ahead prices weighted for total purchases, net of purchases for pumped-
201 storage units, and purchases by neighbouring zones. Additional details on the Italian market
202 structure and the process of the creation of a system marginal price are found in Gianfreda et al.
203 (2016), Gianfreda et al. (2019) and Shah and Lisi (2019).

204 These researchers have emphasised the differences in the generation mix across regions and
205 how the industrial activities are mainly concentrated in the northern area of the country, which
206 is by far the most relevant in terms of consumption, due to the high concentration of population
207 and industries. The northern consumption is 175,396 GWh over 303,443 GWh at the national
208 level. Energy intensity is consistently higher, with an average of 6,326 kWh per inhabitant versus
209 a national average of 5,024 kWh (Terna, 2018). In 2017, the production in the northern zone was
210 149,204 GWh over a total of 289,708 GWh, roughly 51%.

211 The northern area is also characterised by a varied, flexible generation mix, with 26%
212 hydropower, and other renewables such as solar (6%) and biomass (8%); with conventional thermal
213 generation covering the remaining proportion. Yearly details on the evolution of the portfolio
214 generation are reported in Table B.7 in Appendix B, for all zones and across years 2015-2019. At
215 first sight, given the low share of wind, a reader could argue about the choice of selecting Northern
216 Italy to understand the contribution of main drivers to the forecasts of future prices. However,
217 we would like to emphasize that this zone has the highest hydro generation and demand; and
218 more importantly, all three type of thermal, hydro and water pumping units acting in all market
219 sessions. This zone is also connected with four foreign countries, whereas the others have only
220 national connections or limited numbers of foreign connections.

221 Italy has arranged market-coupling agreements with Slovenia since 2011, and with France and
222 Austria since 2015, which represent completion steps to the creation of a single internal electricity
223 market in Europe. Market coupling allows for the simultaneous calculation of electricity prices and
224 cross-border flows across coupled regions, and the main benefits are both an optimised and more

225 efficient utilisation of cross–border capacity and a better price alignment among different countries.
 226 Because of the relevant interconnection capacity between foreign countries and Northern Italy, it
 227 is possible to import electricity at a lower price. For instance, in 2018, Italy imported 47,170
 228 GWh of electricity (approximately equivalent to 15% of total consumption) from French, Swiss,
 229 and Slovenian borders. Table B.8 in Appendix B summarizes the information related to the local
 230 mix, and it reports the technology shares over total installed capacity in neighbouring countries.
 231 Furthermore, the inspection of import/export flows presented in Table 1 shows the relevance of
 232 imports². Hence, cross–border flows are included in this analysis through the construction of
 233 an artificial variable to account for prices determined in interconnected countries and in Central
 234 North, where the local mixes differ substantially. In this way, we do account for their generating
 235 portfolio when using prices weighted by the quantity imported.

Years	France		Austria		Switzerland		Slovenia		Malta		Greece	
	Imports	Exports	Imports	Exports	Imports	Exports	Imports	Exports	Imports	Exports	Imports	Exports
2015	13335	85	1526	33	25263	47	6179	16	0	926	588	1657
2016	11056	286	1420	55	19846	315	6371	16	0	1522	302	1999
2017	10860	280	1313	108	20490	272	5784	23	33	887	325	1614
2018	13102	79	1391	20	21406	122	6707	11	8	606	1053	621
2019	15134	98	1215	1	21231	121	5140	170	18	654	55	3028

Table 1: Italian *Imports from* and *Exports to* other Neighbouring Countries (in GW). Data: ENTSO-E.

236 3. Data and Methodology

237 This section provides a detailed overview of the available data and then explains the
 238 methodological strategy to predict hourly electricity prices. In particular, Subsection 3.1 describes
 239 both the endogenous and the exogenous variables used in our model specifications, while Subsection
 240 3.2 shows all model specifications and the forecast procedure.

241 3.1. Data

242 To perform our analysis, we use day–ahead electricity prices determined hourly in the northern
 243 zone of Italy, and hourly forecasted load, wind and solar generation, actual biomass, waste and

²Details on the dynamics of imports from neighbouring countries over months and across hours are omitted but are available on request.

244 hydropower generated in Northern Italy, together with weighted imports and prices for fossil fuels
245 (coal and natural gas) and CO₂ emissions.

246 Northern Italian zonal prices (in €/MWh) were collected directly from the website of the Italian
247 system operator (*Gestore dei Mercati Energetici*, GME³). Forecasted load, wind and solar were
248 collected from the *European Network of Transmission System Operators for Electricity* (ENTSO-E)
249 and from Refinitiv Thomson Reuters (RTR); and re-scaled from MW to GW.

250 Then, we use both public and private forecasts to compare the forecasting performances of our
251 models. Specifically, we use public ENTSO-E forecast data⁴ from 2015 to 2019; and professional
252 RTR forecasts from 2018 to 2019, since hourly forecasted load, wind and solar were fully available
253 for the northern Italian region only from 2018. In the latter case, we consider the forecasts
254 produced by two weather providers: the *European Centre for Medium-Range Weather Forecast*
255 (ECMWF) and the *Global Forecast System* of the American weather service of the National
256 Centers for Environmental Prediction (GFS). Both providers use two types of weather models - a
257 deterministic one with no involved randomness and a high resolution (the *operational* model), and
258 a probabilistic one with lower resolution but with variations of weather conditions (the *ensemble*
259 model) - and different runs (one run for the *op* and between 21 or 51 runs for the *ens*) at specific
260 hours (namely at midnight, at 6 a.m., at 12 a.m. and at 6 p.m.). Then, according to their ending
261 time of updates and publication, we use two different series of forecasts⁵: one for forecasting models
262 running quickly (*fast*, F), and so including more recent information released at 7.40 a.m.; and one
263 for models running less quickly (*less fast*, LF), then including the information released at 6.55 a.m..
264 These contain the latest information available to market operators to run their forecasting models
265 and formulate their day-ahead bidding strategy of 24 forecasted hourly prices to be submitted (by
266 noon) on the day-ahead market. Hence, in this paper we compare public ENTSO-E with private

³<http://www.mercatoelettrico.org>

⁴This information is published per time unit at the latest two hours before the gate closure time of the day-ahead market or at 12:00 (in local time) at the latest when the gate closure time does not apply. This represents the publication deadline for ENTSOE and actually refers to data available to market operators at (the latest) 10 a.m.

⁵The first series for *fast* models uses forecasts obtained considering first the model ECens00 (which ends its updates at 7.40 a.m.) then any missing forecasts are replaced by the ECop00 (since this ends at 6.55 a.m.), and, if necessary, we use the same replacement scheme using respectively GFSen00, GFSop00, ECen18, ECop18, GFSen18, and GFSop18. Whereas, the second series for *less fast* models simply starts with ECop00. Please note that the runs at 18 were available only from 2018.

267 RTR forecasts to inspect the different forecasting performances.

268 The relevant information for actual biomass, waste and hydro (generated for all 24 hours)
269 and physical flows are collected from ENTSO-E. However, this information is not available in a
270 timely manner for their inclusion in the forecasting models of all the 24 price series, because the
271 quantities usually displayed before noon refer up to hour 11.⁶ Therefore, we consider the lagged
272 actual biomass, waste and hydro generation together with flows for hours from 1 to 10, and their
273 realised values observed at hour 10 for hours 11–24.

274 To construct the *weighted imports*, we use ENTSO-E data for imports and prices of foreign
275 countries. In particular, to consider the effect of imports from foreign countries and from
276 the contiguous zone (Central–Northern Italy), we account for the different prices observed in
277 neighbouring foreign markets and we construct a series of average hourly prices (expressed in
278 €/MWh) *weighted* for the quantity of electricity imported. Specifically, this is calculated as the
279 average of day-ahead hourly prices determined in Austria, France, Switzerland, Slovenia and in
280 Central–Northern Italy, weighted for the actual hourly electricity physical flows, to capture the
281 effects of electricity transits across bordering markets and the neighbouring national zone.

282 Finally, to account for the marginal costs of conventional thermal generation, we use the Dutch
283 TTF natural gas prices (for delivery over the next month), the ICE API2 Rotterdam Future
284 prices for coal and the EEX-EU CO2 emissions E/EUA prices in euros, all collected from RTR
285 Datastream. These prices are settlement prices, released at the end of the day at approximately 7
286 p.m.; hence, included with a time lag $t - 1$.

287 Our final database comprises 35,064 hourly observations for each variable, from January 2015
288 to December 2019; apart from models using RTR forecasted regional data, which cover only 2018
289 and 2019.

290 Following Bunn (2000), Cuaresma et al. (2004) and subsequent references, we adopt a variable
291 segmentation approach. The modelling and forecasting process considers hourly time series per
292 time, i.e. we model and forecast each of the hourly prices individually. Moreover, the model
293 specification strategy replaces missing or incomplete hourly actual data (when they are unavailable
294 because they have not yet been published) with the corresponding information observed for the

⁶The hourly aggregated output are generally published no later than one hour after the operational period, as described by ENTSO-E.

295 same hour on the day before.

296 Differently from Weron (2007) and Afanasyev and Fedorova (2019), we maintain the outliers in
297 all the variable series and we do not decompose the effects of seasonality. We claim that outliers
298 represent peculiar characteristics of the Italian market since they incorporate notable market
299 information in terms of sample variance and arbitrage opportunity from a day-ahead trading
300 perspective. In addition and in contrast to Conejo et al. (2005), Garcia et al. (2005), Weron and
301 Misiorek (2008), Bordignon et al. (2013) among others, we do not apply logarithms to prices to
302 improve normality and stabilize variance, since this transformation could mask the statistical price
303 properties and volatility dynamics that we want to capture and model, see Karakatsani and Bunn
304 (2010) and Paraschiv et al. (2014) for a similar choice.

305 The descriptive statistics of the selected variables are reported in Table 2, and their dynamics
306 are depicted in Figures 1 and 2. Prices show a degree of skewness and a high kurtosis (as for
307 solar, wind and weighted imports). Even if the hourly electricity prices range between 5 and
308 206.12€/MWh, Italian power prices have a floor of 0€/MWh and a cap of 3,000€/MWh. Notably,
309 even if wind generation in Northern Italy exhibits low values (a range between 0 and 20 MW),
310 we include this variable for the sake of generality, completeness and consistency with the local
311 generation mix, as suggested by Ziel et al. (2015); for the same reason, we included biomass and
312 waste. This general approach can be applied to other zones or markets, since it is reasonable to
313 include all fundamental drivers and to expect limited significance of those with lower generation
314 shares. Moreover, it allows for possible changes in the local generation induced by changes in
315 policy regulation or weather conditions.

316 Consumption and electricity prices present weekly and calendar seasonality, with consumption
317 levels higher on working days and lower values during the weekends. These features are more
318 evident in Figure 2, where time series are presented for a sample of hours within peak and off-peak
319 periods (i.e. hours 3, 9, 13, 15, 21, and 24). Consistently, a monthly seasonality is characterised
320 by a consumption peak in winter months (January and February) and a peak in summer months,
321 because of the widespread use of cooling systems and heat pumps. Wind and solar PV generation
322 fluctuate according to weather conditions, and solar PV generation also fluctuates according to
323 hours of solar radiation. Electricity inflows from the bordering central-northern Italian zone
324 and foreign markets (Austria, France, Switzerland, and Slovenia) also exhibit strong seasonality,
325 especially at the beginning of our sample. To help in understanding the effects of these regressors

	Min	Mean	Max	Std.Dev	Skewness	Kurtosis
Price	1.000	52.345	206.120	16.364	1.107	3.426
Forecasted Load	7.344	18.624	31.617	4.858	0.164	-1.107
Weighted Import	0.000	43.075	249.340	15.551	0.911	2.883
Coal	4.280	6.961	9.840	1.598	0.143	-1.350
Natural Gas	9.630	17.575	29.330	3.986	0.296	-0.367
CO ₂	0.440	1.330	3.316	0.877	0.829	-0.937
Forecasted Solar	0.000	0.765	5.499	1.153	1.417	0.832
Forecasted Wind	0.000	0.004	0.035	0.004	1.509	3.623
Hydro	0.550	3.910	10.510	2.029	0.348	-0.772
Biomass	0.044	0.128	0.237	0.036	0.818	-0.013
Waste	0.008	0.037	0.056	0.009	-0.532	0.058

Table 2: Descriptive Statistics of Fundamental Variables computed over the Full Sample. Note that *Std.Dev.* means *standard deviation*.

on prices, their intra-daily dynamics are shown in Figure C.3 in Appendix C.

We consider the Jarque–Bera (JB) test to check for normality of error terms (Jarque and Bera, 1987), and both the augmented Dickey–Fuller (ADF) (Dickey and Fuller, 1979; Said and Dickey, 1984), and the Kwiatkowski–Phillips–Schmidt–Shin (KPSS) tests for the stationarity (Kwiatkowski et al., 1992), and we observed non-normality according to JB test, stationarity according to the ADF test and both level and trend non-stationarity according to the KPSS test. These results for all hours are omitted but available on request.

3.2. Model Specifications

We use several expert- and AR(FI)MA–GARCH–type models.

The first expert specification (EX₁) simply considers past prices observed on one, two and seven days before with weekdays dummies. Formally, the hourly price y_t (for simplicity we omit the subscript h) is modelled as

$$y_t = \alpha + \beta_1 y_{t-1} + \beta_2 y_{t-2} + \beta_3 y_{t-7} + \sum_{k=1}^6 \gamma_k D_t^k + \varepsilon_t \quad (1)$$

where D_t^1 is equal to one for Mondays, D_t^2 for Tuesdays, and so on up to D_t^6 for Saturdays. We

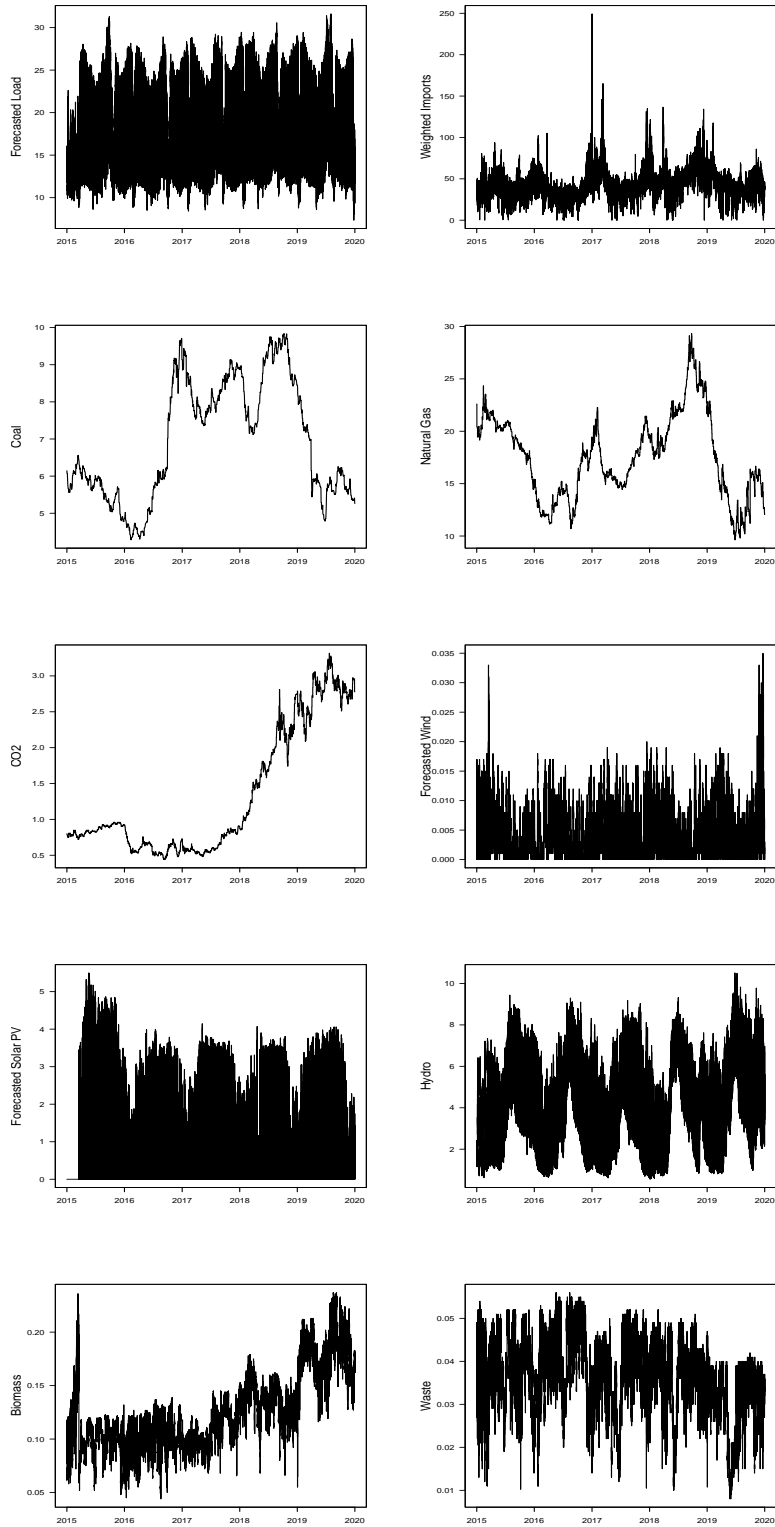


Figure 1: Time Series of all used Exogenous Variables.

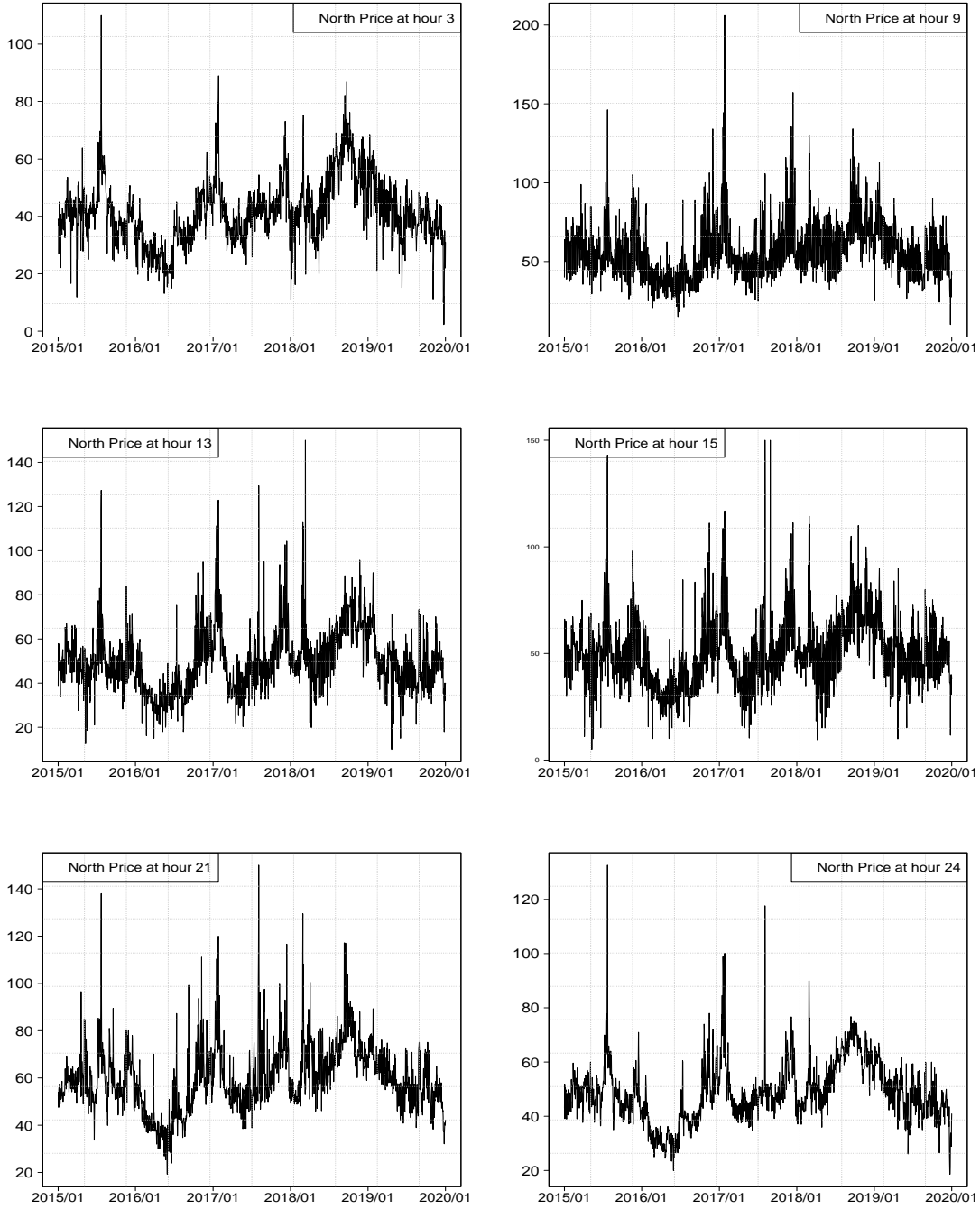


Figure 2: Day-ahead Electricity Prices in Northern Italy at hours 3, 9, 13, 15, 21, and 24.

339 extend this model with a set of exogenous regressors, having the EX_1X defined as

$$y_t = \alpha + \beta_1 y_{t-1} + \beta_2 y_{t-2} + \beta_3 y_{t-7} + \sum_{k=1}^6 \gamma_k D_t^k + \lambda' \mathbf{x}_t + \kappa' \mathbf{z}_{t-1} + \varepsilon_t \quad (2)$$

340 where \mathbf{x}_t is the vector at time t of exogenous regressors, which include forecasted load, wind and

341 solar PV generation, whereas \mathbf{z}_{t-1} is a vector for exogenous regressors at time $t - 1$ since we use
 342 actual hydro, biomass and waste generation, together with weighted imports, natural gas and CO₂
 343 prices.

344 The second expert model (EX₂) builds upon the EX₁ model including the lowest and the highest
 345 hourly prices observed on the previous day, formally

$$y_t = \alpha + \beta_1 y_{t-1} + \beta_2 y_{t-2} + \beta_3 y_{t-7} + \beta_4 y_{min,t-1} + \beta_5 y_{max,t-1} + \sum_{k=1}^6 \gamma_k D_t^k + \varepsilon_t \quad (3)$$

346 As before the EX₂X includes the exogenous regressors \mathbf{x}_t and \mathbf{z}_{t-1} .

347 The third expert model EX₃ expands the EX₂ by including the price at hour 24 of the previous
 348 day (this is omitted when the price at hour 24 is considered)

$$y_t = \alpha + \beta_1 y_{t-1} + \beta_2 y_{t-2} + \beta_3 y_{t-7} + \beta_4 y_{min,t-1} + \beta_5 y_{max,t-1} + \beta_6 y_{24,t-1} + \sum_{k=1}^6 \gamma_k D_t^k + \varepsilon_t \quad (4)$$

349 and, similarly, we have model EX₃X augmented for regressors.

350 The last expert model EX₄ takes into account demeaned prices, formally

$$y_t = \alpha_0 + \alpha_1 \bar{y}_t^w + \sum_{k=1}^8 \beta_k (y_{t-k} - \bar{y}_t^w) + \varepsilon_t \quad (5)$$

351 where \bar{y}_t^w is the mean value of the (hourly) price over the week, and a possible dependency over
 352 the $k = 8$ past days is considered, as in Ziel and Weron (2018). Its augmented variant EX₄X is
 353 expanded by including daily dummies D_t^k (with $k = 1, 2, \dots, 6$ for Mondays, Tuesdays, and so on
 354 to Saturdays) and all exogenous regressors.

355 Moving to the AR(FI)MA models, the first specification is an AR(7), a simple autoregressive
 356 process with 7 lags given by the frequency of our data; and its variant AR(p) with lag length p
 357 estimated over a maximum length size of 7. Formally, our AR(p) models are defined as

$$y_t = \alpha + \sum_{k=1}^4 \beta_s D_t^k + \sum_{j=1}^{11} \gamma_j M_t^j + \sum_{r=1}^p \phi_r y_{t-r} + \varepsilon_t \quad (6)$$

358 with D_t^k , differently from before, being dummies with $k = 1$ for Mondays, $k = 2$ for Saturdays,
 359 $k = 3$ for Sundays, and $k = 4$ for Holidays (not occurring on Saturdays or Sundays); M_t^j are
 360 dummies for months with $j = 1, 2, \dots, 11$ for January, February, \dots , until November, excluding
 361 December. Monthly dummy variables are used to model calendar seasonality, whereas the *Monday* _{t}
 362 dummy captures the impact of a change in consumption among working days and the first day

363 after the weekends. ρ_r with $r = 1, \dots, p$ are the coefficients for the autoregressive terms, with p
364 varying from 1 to 7. If p is fixed to 7, then we have the AR(7) process; differently, if p is estimated
365 from the data, then we have the AR(p) process (details on the estimations are reported in the
366 following section). We also consider their variants augmented for regressors, that is ARX(7) and
367 ARX(p).

368 Then, the autoregressive process is generalized to include moving average components and we
369 consider the general ARMA models with p and q orders, fixed or again estimated from the data.
370 The general formulation for an ARMA(p, q) is

$$y_t = \alpha + \sum_{k=1}^4 \beta_s D_t^k + \sum_{j=1}^{11} \gamma_j M_t^j + \sum_{r=1}^p \phi_r y_{t-r} + \sum_{s=1}^q \theta_s \varepsilon_{t-s} + \varepsilon_t \quad (7)$$

371 with D_t^k dummies with $k = 1$ for Mondays, $k = 2$ for Saturdays, $k = 3$ for Sundays, and
372 $k = 4$ for Holidays, θ_s with $s = 1, \dots, q$ are the coefficients for the moving average terms, with q
373 varying from 1 to 7; and again both are estimated, within a maximum range of 7, that is $p_{max} = 7$
374 and $q_{max} = 7$. For comparisons, we have also considered several specifications of this general
375 process with fixed values, that is: the ARMA(7,7), with $p = q = 7$, the ARMA(7,1) with $p = 7$
376 and $q = 1$, and the ARMA(1,7) with $p = 1$ and $q = 7$. As for the other models, we include
377 in our analysis all ARMAs augmented with exogenous regressors, then testing ARMAX(p, q),
378 ARMAX(7,7), ARMAX(7,1) and ARMAX(7,1).

379 To account for long memory, we finally consider the *autoregressive, fractionally integrated,*
380 *moving-average*, or ARFIMA(p, d, q) models, defined as

$$\Phi(L)(1-L)^d(y_t - \mu_t) = \Theta(L)\varepsilon_t \quad \text{with } \varepsilon_t | \mathcal{F}_{t-1} \sim \mathcal{N}(0, \sigma^2) \quad (8)$$

381 where the normal distribution of the errors has a constant variance, $\sigma^2 \forall t$. d is the fractional
382 integration parameter (with $0 < d < 0.5$) and μ_t is defined as

$$\mu_t = \mu + \sum_{k=1}^4 \beta_s D_t^k + \sum_{j=1}^{11} \gamma_j M_t^j \quad (9)$$

383 with D_t^k dummies with $k = 1$ for Mondays, $k = 2$ for Saturdays, $k = 3$ for Sundays, and
384 $k = 4$ for Holidays; and monthly dummies, M_t^j . As in the ARMA models, we set the p, d, q to be
385 estimated within a range of $p_{max} = 7$, $d_{max} = 2$, and $q_{max} = 7$. We extend this model with our
386 sets of exogenous regressors, obtaining the the ARFIMAX(p, d, q) model, and we compare it with

387 ARFIMAX variants with fixed values for p and q , leaving instead d free to change between 0,1 and
388 2. Specifically, we include in our analysis the ARFIMAX(7,d,7) and the ARFIMAX(7,d,0).

389 Moreover, to account for possible time-varying volatility patterns, asymmetries and shocks
390 induced by fundamental drivers, we expand our models by including GARCH-type specifications.
391 A similar approach has been used by, for example, Koopman et al. (2007), Huurman et al.
392 (2012), Paraschiv et al. (2014), Ketterer (2014), Jeon and Taylor (2016) and Laporta et al. (2018).
393 Therefore, we follow consolidated and well-established modelling approaches.

394 In particular, when the Italian market is considered, Bosco et al. (2007) used an ARMA-
395 GARCH model, whereas Gianfreda and Grossi (2012) used ARFIMAX-GARCHX models.

396 Hence, we compare the performances of several AR(FI)MA models with their variants
397 including GARCH-type specifications, while allowing for an automatic selection of the length
398 of autoregressive and moving average processes and the switching among models, when necessary.
399 To this aim, the considered GARCH specifications are: the *standard* GARCH (SGARCH), the
400 *exponential* GARCH (EGARCH), the *threshold* GARCH (TGARCH), and finally the GARCH-*in-*
401 *mean* (GARCH-M); all with Normal distribution.

402 These models differ according to the type of the GARCH adopted. Thus, the second set of
403 models extends the previous one with time-varying volatility expressed without loss of generality
404 on day t as $\sigma_t^2 = \mathbb{V}(\varepsilon_t | \mathcal{F}_{t-1}) = \text{Var}(\varepsilon_t | \mathcal{F}_{t-1})$. These models are detailed in Appendix A.

405 In particular, the EGARCH(1,1) allows the conditional variance process to respond
406 asymmetrically to rises and falls in electricity prices (Nelson, 1991). To account for asymmetries
407 in volatility, making it a function of positive and negative values of the innovations, we also
408 consider the TGARCH(1,1) process (Zakoian, 1994). Moreover, to consider the possibility that
409 price levels may be influenced by their past price variability and by the fact that volatility in
410 electricity prices is generally stronger when prices are high, we include the standard deviation,
411 as obtained from the conditional variance equation, in the conditional mean equation, adopting
412 the GARCH(1,1)-in-mean (or simply, GARCH-M); as in Kyritsis et al. (2017) and Gianfreda and
413 Scandolo (2018). These GARCH specifications are expanded to include the exogenous regressors
414 \mathbf{x}_t and \mathbf{z}_{t-1} , following the evidence in Huurman et al. (2012) that fundamental drivers improve
415 accuracy when the volatility equation is also included.

416 Finally, we estimate LASSO of further autoregressive models with 28 lags to account for
417 changing market conditions in the last four weeks; their augmented specifications for regressors,

418 that is $AR(28)_{LASSO}$ and $ARX(28)_{LASSO}$; and also the formulation including the time-varying
419 volatility, that is the $ARX(28)$ -GARCHX(1,1)- M_{LASSO} .

420 To summarize, our model set contains 58 models divided in 5 groups: (i) four different
421 *expert* models (EX_1 , EX_2 , EX_3 and EX_4), their extensions with fundamental drivers (EX_1X ,
422 EX_2X , EX_3X and EX_4X) and the EX_4X extended with the time-varying volatility (that is EX_4X -
423 SGARCHX, EX_4X -EGARCHX, EX_4X -TGARCHX and EX_4X -GARCHX-M); (ii) autoregressive
424 AR and ARX models with the order p estimated for the $AR(p)$ and $ARX(p)$, or a priori fixed for
425 the $AR(7)$ with the $ARX(p)$ and $ARX(7)$ extended with the time-varying volatility; (iii) ARMA
426 and ARMAX models where AR and MA lags are estimated or fixed ($ARMA(p,q)$, $ARMA(7,7)$,
427 $ARMA(1,7)$, and $ARMA(7,1)$), their extensions for regressors ($ARMAX(p,q)$, $ARMAX(7,7)$,
428 $ARMAX(1,7)$, and $ARMAX(7,1)$), and their $ARMA(p,q)$ and $ARMA(7,7)$ with the time-varying
429 volatility; (iv) ARFIMA and ARFIMAX models where the AR and MA lags and the fractional
430 integration order are estimated or fixed ($ARFIMA(p,d,q)$, $ARFIMAX(p,d,q)$, $ARFIMAX(7,d,7)$
431 and $ARFIMAX(7,d,0)$), and their extensions with the time-varying volatility; (v) the least absolute
432 shrinkage and selection operator (LASSO) (Tibshirani, 1996) for the AR and ARX models with
433 up to 28 lags and their extension with GARCH-in-mean volatility.

434 3.3. Estimation Methods and Iterative Optimization Procedures

435 The iterative procedure adopted for the selection of the model ordering allows to adapt the
436 price structure to the changing market conditions, as the increasing RES shares in generation,
437 or changes in import/export flows due to additional interconnections, or more generally to agent
438 learning, regulatory and market structural changes. However, to account for possible bias in day-
439 ahead predictions induced by the iterative ordering selection, we compare the iterative models
440 with the ones with ex-ante and pre-determined orders. Let us now describe the iterative model
441 selection process while defining also the estimation and optimization procedures.

442 The iterative model selection is essentially a two-step estimation procedure. In the first step
443 the autoregressive and moving average orders p and q , and (eventually) the fractionally integrated
444 parameter d , are estimated through a grid search process by finding the best model according to
445 the corrected AIC value (AICc), a modification of the original AIC for small sample sizes. The
446 maximum values of the orders are set to 7 in order to consider the 7-day-per-week frequency of
447 our data, so $p_{max} = 7$ and $q_{max} = 7$ respectively, whereas the maximum value of the fractional

448 integration parameter is $d_{max} = 2$.

449 The second step is then used for the ARFIMAX(p,d,q) and the ARMAX(p,q)–GARCHs models,
450 both with exogenous regressors. In the former cases, the estimated orders (\hat{p}, \hat{q}) enter in the
451 ARFIMAX process, and then the fractional integration parameter d is estimated simultaneously
452 with the other parameters of interest. In the latter case, the estimated orders (\hat{p}, \hat{q}) enter in the
453 ARMAX(p,q)–GARCHs processes, and the GARCH orders are estimated simultaneously with the
454 other parameters. For both, we found the *nloptr* nonlinear optimization R package (Johnson, 2021)
455 to be suitable for estimating these type of models. Due to convergence problems in some specific
456 cases and in order to ensure the invertibility of the processes, we changed the numeric tolerance
457 of the solver, or, alternatively, tried a combination of other different solvers. Finally, the model
458 parameters are all estimated by maximum likelihood.

459 Models with fixed orders are instead estimated without any adaptive scheme, due to the ex-
460 ante pre-determined specified orders. In these situations, the estimation procedure is based on
461 conditional sum of squares to find the starting values and then on the maximum likelihood, with the
462 use of the Broyden–Fletcher–Goldfarb–Shanno (BFGS) algorithm for optimization; see Broyden
463 (1970), Fletcher (1970), Goldfarb (1970), Shanno (1970). As before, if convergence problems
464 occur, the procedure allows to fit the model via maximum likelihood and the optimization via a
465 modification of the Simulated Annealing (SANN) of Bélisle (1992), which always guarantees the
466 convergence even with non-differentiable functions, but it can be relatively slow.

467 As far as the LASSO is concerned, we proceed in a way that the relevant exogenous regressors \mathbf{x}_t
468 and \mathbf{z}_{t-1} , combined with the autoregressive terms up to 28 earlier periods, i.e. \mathbf{y}_{t-h} $h = 1, \dots, 28$,
469 are selected by considering a simple linear model. In this way, we are able to properly define
470 a potential subgroup of regressors and autoregressive terms selected at each iteration and for
471 each hour. The criterion used for the statistical bias–variance trade–off, which determines the
472 tuning/penalty parameter, is the *standard cross-validation (cv)* that minimizes the average error.

473 All computations have been executed using the software R and using an AMD EPYC 7542
474 32-Core 2.90 GHz Processor.

475 3.4. Assessment of the Forecasting Performance

476 We compare different model specifications for modelling and forecasting the electricity zonal
477 prices observed over individual hours: each hour is modelled separately by following a daily

478 frequency for prices and drivers. Because all information is available or reconstructed at
479 approximately 11 a.m. (i.e. before the market closure when traders must submit their offers),
480 we are able to model all the 24 hours and forecast them for the next day by a simple prediction
481 process that produces a set of 24 price forecasts for the 24 hours of the following day.

482 We use the first 730 days of our dataset (i.e. from 1/1/2015 to 31/12/2016) for the in-sample
483 estimation, and then the first out-of-sample prediction is obtained for 1/1/2017. Thereafter, the
484 window is rolled one step-ahead with further estimation and forecasts obtained for 2/1/2017, and
485 so forth, until the last observation in the sample. Therefore, we produce forecasts over three years
486 from 1/1/2017 to 31/12/2019, using the ENTSO-E forecasted data. We recall that the modelling
487 and forecasting process is undertaken on day t to provide a set of 24 hourly prices forecasted for
488 the next day $t + 1$. These forecasts must be submitted before the closure of the market, i.e. before
489 noon on day t (thus, we assume that these models have to complete their runs before noon). To
490 predict the day-ahead hourly price on day $t + 1$, we use the information referred to that specific
491 hour as follows: we assume that market operators submit their bids by noon on day t , based
492 on predicted prices for day $t + 1$, obtained by considering fuel prices determined on day $t - 1$;
493 the forecasted values for RES and zonal load available on day t ; the hydro generation, weighted
494 imports, biomass and waste observed on day $t - 1$ for hours 1–10 and their realised values observed
495 at hour 10 on the day t for modelling and forecasting electricity prices of hours 11–24 on day $t + 1$.
496 Indeed, Maciejowska and Nowotarski (2016) and Ziel (2016) note and suggest that prices for early
497 morning hours depend more on the latest information than on information contained at the same
498 hour but on the previous day.

499 To assess the forecasting performance of implemented models, we use both point and density
500 metrics, as the root mean square error (RMSE) and the the continuous ranked probability score
501 (CRPS); see for example Gneiting and Ranjan (2011) and Groen et al. (2013) for early applications
502 in economics, and Gianfreda et al. (2020) for an application to Italian electricity prices. In addition,
503 we implement the one-sided Diebold–Mariano (DM) test to judge the superiority among two
504 competing models (see Diebold and Mariano, 1995 and also West, 1996), and the Hansen–Luden–
505 Nason procedure of Model Confidence Set (MCS) to verify the statistical significance in terms of
506 differences in forecasting performances among the selected models (Hansen et al., 2011). The DM
507 test compares the forecast residuals of only two competing models, and the MCS procedure is a
508 sequence of statistical tests in which the null hypothesis is built on the equal predictive ability

509 (EPA) of several model specifications. Given that the EPA statistical tests can be calculated for
510 different loss functions (depending on the aim of the comparison), we consider a *loss function for*
511 *level* forecasts because of our interest in a comparison of the predictability power in the mean
512 between our models. We also consider a comparison in terms of the full density forecasts by
513 applying the DM and MCS tests to the CRPS metrics.

514 Finally, we compare the forecasting ability of the best performing model when the RTR
515 professional forecasts for consumption, wind and solar replace the ones provided by ENTSO-E. In
516 this latter analysis, the in-sample estimation considers only 365 observations for 2018 and produces
517 forecasts for the whole 2019, because of the reduced size of RTR Italian regional forecasts.

518 4. Results

519 To judge the quality of the forecasted prices, RMSEs and CRPSs are computed and presented
520 in Tables 3 and 4, which also include the Superior Set of Models and the DM tests. These results
521 refer to hours 3, 9, 11, 13, 19, and 21, to the average metrics computed over the 24 hours (Avg_{1-24})
522 and over the peak hours 8–20 (Avg_{8-20}). Results for other hours are omitted but are available on
523 request.

524 Firstly, we observe that the inclusion of exogenous regressors reduces both the RMSEs and the
525 CRPSs, especially during peak hours. Therefore, we extend the empirical evidence in Gianfreda
526 et al. (2020) on the predictive power of a large set of exogenous regressors to forecast, this time,
527 regional prices; whereas, the *single national prices* were forecasted in the cited reference.

528 Considering the whole set of 58 models, it can be easily observed that the expert EX₄X model
529 drastically outperform all other models in point forecasts, with the lowest average errors of around
530 7 and 6 €/MWh over peak and base periods, respectively. These results clearly declare the
531 EX₄X model as the superior specification in point forecasting. Interestingly, including a time-
532 varying variance does not significantly increase the point forecasting accuracy of these Italian
533 zonal prices; however, in general some potential improvements can be expected as discussed in Ziel
534 et al. (2015)). The other AR(FI)MA models provide higher and similar errors, even if they differ
535 in their structures.

536 Notably, the forecasting precision drastically decreases during the ramp-up and ramp-down
537 phases (hours 9 and 19), when the conventional thermal generation is necessary to restore the
538 balance between demand and supply. Across peak hours, the non programmable renewables

539 (especially solar and wind) bid at 0 €/MWh and have priority of dispatch of the produced energy.
540 Therefore, their intermittent, erratic in-feed increases the variability of prices and consequently
541 affects the forecasting errors, especially when demand is at its higher levels (at hours 9 and 19).

542 Furthermore, the predictability power of fundamental variables decreases during the evening
543 hours because the forecast horizons are longer than those for the morning hours. This argument is
544 particularly notable for RES because the accuracy of weather predictions decreases substantially
545 with the length of forecasting horizons.

546 There are no substantial improvements when LASSO models are considered. Therefore, based
547 on this evidence and on previous explorations⁷, we conclude that the LASSO is not necessary to
548 improve accuracy in our context, characterized by a limited number of regressors with respect to
549 the amount of statistical information available.

550 Indeed, when all models are simultaneously compared, the computations of the Superior Set
551 of Models⁸, in terms of minimum loss function for level forecasts, show that the LASSO models
552 are always discarded. Moreover, none of the models provide more accurate forecasts than those of
553 the EX₄X, which is considered as the benchmark in the one-sided DM tests (under the alternative
554 hypothesis that any other model is more accurate than the EX₄X). This model is always retained
555 in the Superior Set of Models and also the DM tests confirm its out-performance in pairwise
556 comparisons. More importantly for a practical point of view, this expert model and its GARCH
557 variants are the only ones retained for all hours in the MCS, and especially when hour 19 is
558 considered. Hence, market operators willing to adopt a single model to forecast all hourly prices
559 should consider this relevant and so clearly assessed fact.

560 For completeness, we extend the analysis to density forecasting and investigate if a more general
561 loss function provide different evidence. Looking at Table 4, results on CRPS show that there
562 are substantial improvements when all models are enlarged to include the GARCH time-varying

⁷In previous analyses on LASSO specifications, we note that on average LASSOs perform better when considering the simultaneous selection of the autoregressive terms with the exogenous regressors, revealing that not all the lagged terms are useful at each iteration. Moreover, including exogenous regressors both in the conditional mean and conditional variance does not improve on average the power predictability of the same model.

⁸We implement the MCS procedure with the $T_{max, \mathcal{M}}$ test (Hansen et al., 2011, p. 465) at the $\alpha = 0.15$ significance level by using the R function `MCSprocedure` within the package `MCS` written by Bernardi and Catania (2018).

563 volatility. Indeed, the average of CRPS over the 24 hours of all the models with time-varying
564 volatility is in the range 0.156-0.160, whereas the same average for models without time-varying
565 volatility is around 0.3. Specifications for only the conditional mean are always excluded from
566 the MCS, apart for the $AR(28)_{LASSO}$, which however does provide forecasts not statistically more
567 accurate than the benchmark EX_4X in the DM tests. The expert models augmented with time-
568 varying volatility are the only (class of) models that is never excluded from the MCS. Moreover,
569 the DM tests show that generally all GARCHs specifications are statistically superior to the
570 benchmark, confirming the importance of including the time-varying volatility. Therefore, when
571 the loss function is generalized to the full distribution, sophisticated specifications that allow for
572 time-varying volatility are essential to improve the forecast accuracy.

573 Given the focus on forecasting, we compare the forecasting performance of the EX_4X and
574 EX_4X -SGARCHX models when professional and more timely forecasts are used in place of public
575 and freely available forecasts. The RMSEs and CRPSs for a selection of hours and averages over
576 base and peak hours are presented in Tables 5 and 6. However, to show in full the performance of
577 these models, we have decided to report results for all 24 hours in Tables B.9 and B.10 in Appendix
578 B.

579 We compare the forecasting performances of EX_4X when ENTSO-E forecasts are considered,
580 with those obtained by the same model when instead RTR forecasts are used. As anticipated,
581 these professional forecasts are released more timely and represent the best updated information
582 available at 6.55 and at 7.40 a.m. when market operators can start running their forecasting models
583 to formulate their day-ahead bidding strategy. Then, we distinguish between models which can
584 run quickly (and their forecasts are labelled with F for *fast*), from those running less quickly (hence
585 labelled with LF for *less fast*). In our case, we compare the forecasting performances of EX_4X -
586 F and EX_4X -LF with EX_4X and the ones from EX_4X -SGARCHX-F and EX_4X -SGARCHX-LF
587 with EX_4X -SGARCHX. Also for this exercise, we have studied other model specifications with
588 professional forecasts and results are qualitative similar. Then, we emphasize that the evidence is
589 not driven by considering simple or complex models, but by the usage of professional forecasts.

590 Results clearly show that using professional forecasts improves substantially price forecasts,
591 especially during hours 1-7, and peak hours 8-20. Then, as soon as the forecasting horizon increases,
592 as after hour 21, the benefits of using professional forecasts disappear. Moreover, in the very short-
593 horizon up to hour 18, there is no difference between the two forecasting models running with the

594 latest information: indeed *fast* and *less fast* models perform equivalently. They diverge when the
595 fast model shows better (but small) gains at hour 19, before losing any forecasting power as soon
596 as the forecasting horizon further increases to hours 21-24. Therefore, these results emphasize
597 the importance of implementing forecasting models with accurate and professionally computed
598 forecasts; and, if possible, traders should wait for the latest published forecasts to take longer
599 benefits of the forecasting gain. Even in this case, GARCH specifications do not substantially
600 improve the point forecasts, whereas the opposite occurs for the density forecasts. And the take
601 home messages are that traders and market operators are encouraged to use models accounting for
602 higher moments of the distributions, as suggested in Gianfreda and Bunn (2018), while considering
603 professional forecasts.

604 Finally, in what follows, we discuss the estimated coefficients (with confidence intervals at 90%)
605 of the EX₄X model. Results generally refer to hours 3, 9, 15, and 21 in the out-of-sample period.
606 However, some additional hours are considered with respect to the intra-daily profiles of drivers,
607 and results for the remaining hours are omitted but are available upon request.

608 Consistently with the literature, forecasted load is statistically significant with a positive effect
609 on day-ahead price, meaning that prices do respond to load as shown in Figure C.4 in Appendix
610 C. However, for hour 3, we document an increasing influence in 2018, then decreasing in 2019.
611 Hours 9 and 15 show different dynamics with an almost constant influence until the end of 2018
612 but a substantial lower and progressively decreasing influencing power over the whole 2019, which
613 may reflect the *negative demand* effect played by solar PV generation according to its generation
614 and new additions. Whereas, hour 21 exhibits a decreasing influence already from July 2017,
615 probably for more conventional power available to cover demand (and so being less at the margin).

616 The estimated coefficients for solar PV forecasts are depicted in Figure C.5, and it shows that
617 it is statistically significant at hours 13 and 15 with a negative sign, implying the reduction of
618 the mean level of zonal prices. At hour 9 or 11 when sun starts to shine, it turns from significant
619 to non significant from the last part of 2017 or middle 2018 and through all the other years.
620 Notwithstanding the limited generation in northern Italy, forecasted wind is found to have a
621 significant negative effect at hour 3, whereas its effect turns from significant to non significant
622 from roughly the beginning of 2018 at hours 9 and 21. Instead, it is found almost never significant
623 at hour 15; see Figure C.6.

624 Looking at hydro and its intra-daily profile, we were expecting significant (negative) effects at

625 hours 9 and 21 when its generation is at its maximum. Whereas, the estimated coefficients for
626 actual hydropower generation is not found statistically significant at these hours. Figure C.7 shows
627 that it is found statistically significant only at hour 3, when it does not suffer the competition of
628 solar PV (and wind to less extent).

629 As far as weighted imports are considered, they are not found to be significant (as reported at
630 hours 3, 9, 15 and 21), see Figure C.10. Therefore, foreign prices and imported quantities seem
631 not to affect northern Italian electricity price via scheduled capacity on interconnectors. The same
632 conclusion is drawn for biomass and waste. Coal is instead found to be significant only at hour 15
633 and up to the beginning of 2018, then it turned out to be misplaced by the progressive penetration
634 of RES. Figure C.12 shows that natural gas confirms its attitude to increase electricity prices at
635 hour 3. This finding is surprising considering the relevant share of electricity generation covered
636 by combined cycle gas turbine plants in northern Italy. Similarly, also CO₂ emission prices exhibit
637 an almost never significant effect, see Figure C.13.

638 However, it must be noted that these conclusions on the dynamics of coefficients for exogenous
639 regressors are based on a model accounting for the dependence of prices over the previous 8
640 demeaned prices. Then, the model seems 'expert' enough with the inclusion of past essential
641 information together with the contribution of load, wind, solar, hydro and natural gas.

Models	3	9	11	13	19	21	Avg ₈₋₂₀	Avg ₁₋₂₄
EX ₁	6.468	12.501	10.822	9.834	11.836	8.911	10.973	9.150
EX ₂	6.437	12.162	10.533	9.636	11.748	8.809	10.760	9.016
EX ₃	5.984	11.960	10.309	9.411	11.804	8.756	10.616	8.824
EX ₄	5.204	9.469	8.284	7.998	8.365	6.643	8.516	7.074
EX ₁ X	6.151	11.691	10.196	9.144	11.169	8.614	10.303	8.644
EX ₂ X	6.113	11.563	10.062	9.062	11.175	8.636	10.237	8.602
EX ₃ X	5.814	11.378	9.864	8.895	11.237	8.756	10.131	8.499
EX ₄ X	4.860	8.691	7.708	7.318	8.106	6.466	7.871	6.615
EX ₄ X-SGARCHX	4.861	8.834	7.712	7.274	8.284	6.449	7.919	6.628
EX ₄ X-EGARCHX	4.912	8.790	7.805	7.230	8.207	6.473	7.907	6.626
EX ₄ X-TGARCHX	4.894	8.835	7.791	7.286	8.401	6.595	7.992	6.689
EX ₄ X-GARCHX-M	4.925	8.846	7.788	7.313	8.264	6.420	7.976	6.662
AR(7)	5.577	11.500	9.867	9.228	10.272	8.122	10.130	8.327
AR(p)	5.529	11.977	10.170	9.545	10.521	8.223	10.582	8.596
ARX(7)	5.489	10.706	9.162	8.521	9.932	7.837	9.412	7.847
ARX(p)	5.449	11.000	9.428	8.739	10.135	7.871	9.703	8.024
ARX(7)-SGARCHX	5.462	10.722	9.177	8.337	9.739	7.689	9.367	7.795
ARX(7)-EGARCHX	5.462	10.873	9.225	8.455	9.712	7.786	9.395	7.826
ARX(7)-TGARCHX	5.506	10.596	9.208	8.489	10.048	7.745	9.472	7.871
ARX(7)-GARCHX-M	5.470	10.692	9.184	8.348	9.804	7.689	9.405	7.843
ARX(p)-SGARCHX	5.436	10.924	9.404	8.591	10.088	7.777	9.736	8.034
ARX(p)-EGARCHX	5.446	11.074	9.536	8.618	10.021	7.899	9.720	8.030
ARX(p)-TGARCHX	5.498	11.001	9.484	8.979	10.309	7.837	9.932	8.164
ARX(p)-GARCHX-M	5.468	11.025	9.571	8.603	10.091	7.813	9.824	8.114
ARMA(7,7)	5.717	13.542	10.430	9.402	10.629	9.974	10.615	8.934
ARMA(1,7)	5.589	11.808	9.942	9.362	10.449	8.192	10.309	8.447
ARMA(7,1)	5.584	11.483	9.821	9.191	10.310	8.105	10.091	8.300
ARMA(p,q)	5.561	11.805	10.066	9.429	10.520	8.160	10.450	8.516
ARMAX(7,7)	5.533	10.418	9.197	8.493	9.950	7.685	9.339	7.824
ARMAX(1,7)	5.518	10.770	9.176	8.571	10.003	7.819	9.444	7.873
ARMAX(7,1)	5.494	10.710	9.136	8.498	9.968	7.832	9.394	7.836
ARMAX(p,q)	5.467	10.959	9.353	8.660	10.129	7.827	9.630	7.975
ARMAX(7,7)-SGARCHX	5.693	10.562	10.574	8.461	9.831	7.893	9.708	8.044
ARMAX(7,7)-EGARCHX	5.578	12.429	9.732	8.662	9.827	8.050	9.702	8.045
ARMAX(7,7)-TGARCHX	5.624	10.768	9.261	8.762	10.003	7.752	9.495	7.910
ARMAX(7,7)-GARCHX-M	5.689	10.746	9.228	8.530	9.959	7.719	9.519	8.135
ARMAX(p,q)-SGARCHX	5.453	10.867	9.314	8.649	10.060	7.737	9.625	7.959
ARMAX(p,q)-EGARCHX	5.456	10.875	9.376	8.522	10.138	7.779	9.626	8.009
ARMAX(p,q)-TGARCHX	5.507	10.959	9.248	8.638	10.303	7.822	9.781	8.060
ARMAX(p,q)-GARCHX-M	5.501	11.157	9.526	8.766	10.112	7.756	9.991	8.195
ARFIMA(p,d,q)	5.572	11.261	9.827	9.267	10.054	8.223	10.063	8.289
ARFIMAX(p,d,q)	5.467	10.959	9.353	8.661	10.121	7.827	9.630	7.975
ARFIMAX(p,d,q)-SGARCHX	5.459	10.847	9.303	8.620	10.044	7.762	9.617	7.947
ARFIMAX(7,d,7)-SGARCHX	5.604	10.782	9.134	8.462	10.064	7.799	9.513	7.923
ARFIMAX(7,d,0)-SGARCHX	5.455	10.806	9.143	8.317	9.895	7.698	9.385	7.804
ARFIMAX(p,d,q)-EGARCHX	5.468	10.807	9.482	8.678	10.132	7.745	9.653	7.975
ARFIMAX(7,d,7)-EGARCHX	5.763	10.655	9.828	10.534	10.007	8.823	9.703	8.110
ARFIMAX(7,d,0)-EGARCHX	5.458	10.727	9.064	8.473	9.775	7.749	9.354	7.796
ARFIMAX(p,d,q)-TGARCHX	5.480	11.010	9.247	8.543	10.213	7.782	9.702	8.007
ARFIMAX(7,d,7)-TGARCHX	5.588	10.447	9.217	8.664	9.895	7.780	9.424	7.884
ARFIMAX(7,d,0)-TGARCHX	5.506	10.671	9.110	8.383	10.009	7.689	9.400	7.833
ARFIMAX(p,d,q)-GARCHX-M	5.480	10.999	9.424	8.671	10.178	7.839	10.068	8.262
ARFIMAX(7,d,7)-GARCHX-M	6.586	10.883	9.334	8.595	10.209	7.962	9.913	8.402
ARFIMAX(7,d,0)-GARCHX-M	5.480	10.782	9.084	8.289	10.021	7.714	9.436	7.852
AR(28) _{LASSO}	6.415	12.395	10.802	9.960	11.462	9.007	10.914	9.117
ARX(28) _{LASSO}	6.197	11.736	10.094	9.210	11.051	8.649	10.259	8.636
AR(28)-GARCH-M _{LASSO}	6.394	12.614	10.845	10.045	11.859	9.171	11.143	9.275
ARX(28)-GARCHX-M _{LASSO}	6.295	11.577	10.258	9.195	11.060	8.678	10.361	8.721

Table 3: RMSEs of all selected models and for a section of hours. The average over the 24 hours and the average over peak hours 8-20 are also included. Grey cells refer to specifications excluded from the Superior Set of Models selected according to the Hansen-Luden-Nason MCS procedure at $\alpha = 0.15$. ***, ** and * indicate that a model is more accurate than the EX₄X benchmark model at the 0.1%, 1%, 5% significance levels according to the one-sided DM test. Absence of stars indicates that none of the alternative specifications provides more accurate forecasts.

Models	3	9	11	13	19	21	Avg ₈₋₂₀	Avg ₁₋₂₄
EX ₁	0.255	0.332	0.317	0.298	0.323	0.313	0.317	0.298
EX ₂	0.254	0.332	0.318	0.299	0.323	0.313	0.317	0.298
EX ₃	0.253	0.333	0.318	0.300	0.324	0.313	0.318	0.298
EX ₄	0.252	0.323	0.309	0.291	0.314	0.309	0.309	0.292
EX ₁ X	0.254	0.327	0.312	0.294	0.319	0.314	0.312	0.295
EX ₂ X	0.253	0.327	0.312	0.294	0.319	0.314	0.312	0.295
EX ₃ X	0.253	0.327	0.312	0.294	0.320	0.313	0.313	0.295
EX ₄ X	0.251	0.320	0.307	0.289	0.313	0.308	0.307	0.290
EX ₄ X-SGARCHX	0.125***	0.199***	0.174***	0.156***	0.178***	0.166***	0.178	0.158
EX ₄ X-EGARCHX	0.125***	0.198***	0.173***	0.155***	0.180***	0.164***	0.178	0.158
EX ₄ X-TGARCHX	0.124***	0.199***	0.174***	0.155***	0.178***	0.167***	0.179	0.158
EX ₄ X-GARCHX-M	0.125***	0.201***	0.173***	0.155***	0.178***	0.164***	0.179	0.158
AR(7)	0.254	0.326	0.312	0.294	0.317	0.312	0.312	0.295
AR(p)	0.252	0.324	0.310	0.292	0.314	0.309	0.310	0.292
ARX(7)	0.252	0.323	0.309	0.292	0.315	0.310	0.309	0.292
ARX(p)	0.252	0.324	0.310	0.292	0.314	0.310	0.310	0.293
ARX(7)-SGARCHX	0.124***	0.201***	0.176***	0.158***	0.177***	0.163***	0.179	0.158
ARX(7)-EGARCHX	0.124***	0.205***	0.179***	0.159***	0.177***	0.166***	0.181	0.159
ARX(7)-TGARCHX	0.124***	0.200***	0.175***	0.154***	0.179***	0.162***	0.178	0.158
ARX(7)-GARCHX-M	0.124***	0.201***	0.175***	0.158***	0.177***	0.163***	0.179	0.158
ARX(p)-SGARCHX	0.124***	0.200***	0.174***	0.153***	0.176***	0.163***	0.177	0.157
ARX(p)-EGARCHX	0.124***	0.208***	0.179***	0.156***	0.177***	0.166***	0.181	0.160
ARX(p)-TGARCHX	0.124***	0.201***	0.173***	0.149***	0.177***	0.161***	0.176	0.156
ARX(p)-GARCHX-M	0.124***	0.201***	0.175***	0.154***	0.176***	0.163***	0.178	0.158
ARMA(7,7)	0.264	0.341	0.326	0.308	0.328	0.324	0.326	0.307
ARMA(1,7)	0.264	0.338	0.324	0.307	0.328	0.322	0.324	0.306
ARMA(7,1)	0.264	0.338	0.324	0.307	0.328	0.322	0.324	0.306
ARMA(p,q)	0.262	0.337	0.323	0.305	0.327	0.320	0.323	0.304
ARMAX(7,7)	0.252	0.323	0.310	0.292	0.315	0.310	0.310	0.292
ARMAX(1,7)	0.261	0.335	0.321	0.303	0.326	0.319	0.321	0.303
ARMAX(7,1)	0.252	0.323	0.309	0.292	0.315	0.310	0.309	0.292
ARMAX(p,q)	0.261	0.335	0.321	0.303	0.326	0.319	0.321	0.303
ARMAX(7,7)-SGARCHX	0.125***	0.202***	0.179***	0.157***	0.180***	0.165***	0.180	0.159
ARMAX(7,7)-EGARCHX	0.126***	0.203***	0.183***	0.159***	0.179***	0.166***	0.182	0.160
ARMAX(7,7)-TGARCHX	0.125***	0.201***	0.178***	0.156***	0.180***	0.163***	0.180	0.159
ARMAX(7,7)-GARCHX-M	0.125***	0.202***	0.177***	0.158***	0.178***	0.164***	0.181	0.159
ARMAX(p,q)-SGARCHX	0.124***	0.202***	0.176***	0.157***	0.178***	0.163***	0.179	0.158
ARMAX(p,q)-EGARCHX	0.124***	0.206***	0.179***	0.157***	0.177***	0.166***	0.181	0.159
ARMAX(p,q)-TGARCHX	0.124***	0.201***	0.175***	0.152***	0.179***	0.161***	0.178	0.157
ARMAX(p,q)-GARCHX-M	0.124***	0.202***	0.176***	0.158***	0.177***	0.163***	0.179	0.158
ARFIMA(p,d,q)	0.263	0.339	0.325	0.307	0.328	0.321	0.325	0.306
ARFIMAX(p,d,q)	0.261	0.335	0.321	0.303	0.326	0.319	0.321	0.303
ARFIMAX(p,d,q)-SGARCHX	0.124***	0.201***	0.175***	0.157***	0.178***	0.164***	0.178	0.158
ARFIMAX(7,d,7)-SGARCHX	0.125***	0.202***	0.178***	0.158***	0.179***	0.164***	0.181	0.160
ARFIMAX(7,d,0)-SGARCHX	0.125***	0.201***	0.176***	0.158***	0.177***	0.163***	0.179	0.158
ARFIMAX(p,d,q)-EGARCHX	0.125***	0.206***	0.179***	0.158***	0.177***	0.166***	0.181	0.160
ARFIMAX(7,d,7)-EGARCHX	0.126***	0.204***	0.182***	0.161***	0.179***	0.167***	0.183	0.161
ARFIMAX(7,d,0)-EGARCHX	0.125***	0.205***	0.179***	0.159***	0.178***	0.167***	0.181	0.160
ARFIMAX(p,d,q)-TGARCHX	0.124***	0.200***	0.176***	0.152***	0.179***	0.162***	0.178	0.157
ARFIMAX(7,d,7)-TGARCHX	0.125***	0.200***	0.178***	0.157***	0.179***	0.164***	0.180	0.159
ARFIMAX(7,d,0)-TGARCHX	0.124***	0.200***	0.176***	0.154***	0.179***	0.162***	0.178	0.158
ARFIMAX(p,d,q)-GARCHX-M	0.124***	0.202***	0.175***	0.157***	0.177***	0.163***	0.178	0.158
ARFIMAX(7,d,7)-GARCHX-M	0.126***	0.203***	0.177***	0.158***	0.178***	0.165***	0.180	0.160
ARFIMAX(7,d,0)-GARCHX-M	0.124***	0.201***	0.176***	0.158***	0.177***	0.164***	0.179	0.158
AR(28) _{LASSO}	0.254	0.327	0.313	0.294	0.317	0.312	0.312	0.295
ARX(28) _{LASSO}	0.256	0.327	0.311	0.294	0.318	0.313	0.312	0.295
AR(28)-GARCH-M _{LASSO}	0.124***	0.201***	0.176***	0.158***	0.181***	0.163***	0.179	0.158
ARX(28)-GARCHX-M _{LASSO}	0.125***	0.200***	0.173***	0.153***	0.179***	0.166***	0.178	0.158

Table 4: CRPSs of all selected models and for a section of hours. The average over the 24 hours and the average over peak hours 8-20 are also included. Grey cells refer to specifications excluded from the Superior Set of Models selected according to the Hansen-Luden-Nason MCS procedure at $\alpha = 0.15$. ***, ** and * indicate that a model is more accurate than the EX₄X benchmark model at the 0.1%, 1%, 5% significance levels according to the one-sided DM test. Absence of stars indicates that the alternative specification does not provide more accurate forecasts.

	3	9	11	13	19	21	Avg ₁₋₂₄	Avg ₈₋₂₀
EX ₄ X	5.082	9.782	7.515	6.888	6.719	5.105	6.605	7.814
EX ₄ X-F	4.629*	6.562***	6.325***	5.681***	5.354***	4.668**	5.264	5.938
EX ₄ X-LF	4.624*	6.553***	6.329***	5.694***	5.357***	4.673**	5.266	5.941
EX ₄ X-SGARCHX	5.090	9.939	7.663	7.074	6.739	5.269	6.745	8.031
EX ₄ X-SGARCHX-F	4.592**	6.573***	6.273***	5.525***	5.400***	4.645**	5.302	5.932
EX ₄ X-SGARCHX-LF	4.580**	6.593***	6.307***	5.597***	5.362***	4.647**	5.303	5.937

Table 5: RMSEs of the best performing model with ENTSO-E forecasts (EX₄X and EX₄X-SGARCHX-norm) and with ETR forecasts for *fast* (EX₄X-F and EX₄X-SGARCHX-norm-F) and *less fast* (EX₄X-LF and EX₄X-SGARCHX-norm-LF) models, over 365 forecasts computed for the whole 2019 for a selection of hours. The average over the 24 hours and the average over peak hours 8-20 are also included. Grey cells refer to specifications excluded from the Superior Set of Models selected according to the Hansen-Luden-Nason MCS procedure at $\alpha = 0.15$. ***, ** and * indicate that a model is more accurate than the EX₄X benchmark model at the 0.1%, 1%, 5% significance levels according to the one-sided DM test. Absence of stars indicates that the alternative specification does not provide more accurate forecasts.

	3	9	11	13	19	21	Avg ₁₋₂₄	Avg ₈₋₂₀
EX ₄ X	0.239	0.310	0.301	0.280	0.293	0.295	0.278	0.296
EX ₄ X-F	0.269	0.297***	0.295***	0.307***	0.313***	0.301***	0.285	0.299
EX ₄ X-LF	0.269	0.297***	0.295***	0.307***	0.313***	0.301***	0.285	0.299
EX ₄ X-SGARCHX	0.103***	0.179***	0.164***	0.140***	0.144***	0.134***	0.137	0.159
EX ₄ X-SGARCHX-F	0.098***	0.128***	0.113***	0.117***	0.141***	0.121***	0.112	0.125
EX ₄ X-SGARCHX-LF	0.099***	0.126***	0.112***	0.117***	0.144***	0.122***	0.112	0.125

Table 6: CRPSs of the best performing model with ENTSO-E forecasts (EX₄X and EX₄X-SGARCHX-norm) and with ETR forecasts for *fast* (EX₄X-F and EX₄X-SGARCHX-norm-F) and *less fast* (EX₄X-LF and EX₄X-SGARCHX-norm-LF) models, over 365 forecasts computed for the whole 2019 for a selection of hours. The average over the 24 hours and the average over peak hours 8-20 are also included. Grey cells refer to specifications excluded from the Superior Set of Models selected according to the Hansen-Luden-Nason MCS procedure at $\alpha = 0.15$. ***, ** and * indicate that a model is more accurate than the EX₄X benchmark model at the 0.1%, 1%, 5% significance levels according to the one-sided DM test. Absence of stars indicates that the alternative specification does not provide more accurate forecasts.

642 5. Conclusions

643 Forecasting day-ahead electricity prices has become extremely important for generation
644 planning, given the imperfect predictability of weather conditions that affects both demand and
645 RES generation, and for trading decisions influenced by the exploitation of possible arbitrage
646 opportunities that can occur in subsequent market sessions. Hence, this paper provides a
647 comparison of expert and AR(FI)MA models with GARCH specifications with fixed or estimated
648 structures through a flexible model selection by an iterative and adaptive procedure. Results show
649 that the best performing model is an expert one augmented for exogenous regressors and time-
650 varying volatility, especially if density forecasting has to be assessed. The importance of producing
651 good and timely predictions of hourly day-ahead prices for northern Italy is also tested against
652 the usage of commercial forecasts, since monitoring the bidding strategies for detecting strategic
653 behaviours across market sessions is becoming crucial to avoid market speculations and consequent
654 increasing costs for final customers.

655 Using a set of drivers, including forecasted demand, forecasted wind and solar PV generation,
656 fossil fuels, and actual hydro, biomass and waste generation together with price-weighted flows,
657 northern Italian electricity prices are forecasted through linear and nonlinear models, some of them
658 with a flexible structure iteratively selected at both the autoregressive and moving average orders
659 over each calibration window, including the possibility to switch from one model to another one.
660 Our results clearly show that if point forecasts are of concern a simple expert model overcomes
661 all other specifications, and that adopting a flexible structures changing with time-varying market
662 conditions and avoiding over-parametrisation in an ex-ante ordering selection performs equally
663 well, although is not recommended for all hours.

664 We provide evidence that fundamental factors can drive zonal electricity prices differently
665 within trading periods and that their simultaneous inclusion (fuels, imports and RES as well)
666 substantially improves the forecast accuracy. However, when studying the density forecasting,
667 only nonlinear models that allow for time-varying volatility and second-moment dynamics provide
668 more accurate results. Finally, we find that using professional and more timely consumption and
669 RES predictions improves the forecast accuracy of electricity prices more than using predictions
670 freely available to researchers.

671 **References**

- 672 Abramova, E. and Bunn, D. (2020). Forecasting the intra-day spread densities of electricity prices.
673 *Energies*, 13(3).
- 674 Afanasyev, D. O. and Fedorova, E. A. (2019). On the impact of outlier filtering on the electricity
675 price forecasting accuracy. *Applied energy*, 236:196–210.
- 676 B elisle, C. J. (1992). Convergence theorems for a class of simulated annealing algorithms on rd.
677 *Journal of Applied Probability*, pages 885–895.
- 678 Bernardi, M. and Catania, L. (2018). The model confidence set package for R. *International*
679 *Journal of Computational Economics and Econometrics*, 8(2):144–158.
- 680 Bernardi, M. and Lisi, F. (2020). Point and interval forecasting of zonal electricity prices and
681 demand using heteroscedastic models: The ipex case. *Energies*, 13(23).
- 682 Bordignon, S., Bunn, D. W., Lisi, F., and Nan, F. (2013). Combining day-ahead forecasts for
683 British electricity prices. *Energy Economics*, 35:88 – 103.
- 684 Bosco, B. P., Parisio, L. P., and Pelagatti, M. M. (2007). Deregulated wholesale electricity prices
685 in Italy: an empirical analysis. *International Advances in Economic Research*, 13(4):415–432.
- 686 Broyden, C. G. (1970). The convergence of a class of double-rank minimization algorithms: 2. the
687 new algorithm. *IMA journal of applied mathematics*, 6(3):222–231.
- 688 Bunn, D. W. (2000). Forecasting loads and prices in competitive power markets. In *Proceedings*
689 *of the IEEE*, volume 88, pages 163–169.
- 690 Bunn, D. W., Gianfreda, A., and Kermer, S. (2018). A trading-based evaluation of density forecasts
691 in a real-time electricity market. *Energies*, 11(10).
- 692 Chen, D. and Bunn, D. (2014). The forecasting performance of a finite mixture regime-switching
693 model for daily electricity prices. *Journal of Forecasting*, 33(5):364–375.
- 694 Conejo, A. J., Contreras, J., Espinola, R., and Plazas, M. A. (2005). Forecasting electricity prices
695 for a day-ahead pool-based electricity energy market. *International Journal of Forecasting*,
696 21(3):435–462.

697 Cuaresma, J. C., Hlouskova, J., Kossmeier, S., and Obersteiner, M. (2004). Forecasting electricity
698 spot-prices using linear univariate time-series models. *Applied Energy*, 77(1):87 – 106.

699 de Marcos, R. A., Bello, A., and Reneses, J. (2019). Electricity price forecasting in the short
700 term hybridising fundamental and econometric modelling. *Electric Power Systems Research*,
701 167:240–251.

702 Dickey, D. A. and Fuller, W. A. (1979). Distribution of the estimators for autoregressive time
703 series with a unit root. *Journal of the American statistical association*, 74(366a):427–431.

704 Diebold, F. X. and Mariano, R. S. (1995). Comparing predictive accuracy. *Journal of Business &
705 Economic Statistics*, 13(3):253–263.

706 Fletcher, R. (1970). A new approach to variable metric algorithms. *The computer journal*,
707 13(3):317–322.

708 Garcia, R. C., Contreras, J., van Akkeren, M., and Garcia, J. (2005). A GARCH forecasting model
709 to predict day-ahead electricity prices. *IEEE Transactions on Power Systems*, 20(2):867–874.

710 Gianfreda, A. and Bunn, D. (2018). A stochastic latent moment model for electricity price
711 formation. *Operations Research*, 66:1189–1456.

712 Gianfreda, A. and Grossi, L. (2012). Forecasting Italian electricity zonal prices with exogenous
713 variables. *Energy Economics*, 34(6):2228 – 2239.

714 Gianfreda, A., Parisio, L., and Pelagatti, M. (2018). A review of balancing costs in Italy before
715 and after RES introduction. *Renewable and Sustainable Energy Reviews*, 91:549–563.

716 Gianfreda, A., Parisio, L., and Pelagatti, M. (2019). The RES-induced switching effect across fossil
717 fuels: An analysis of day-ahead and balancing prices. *Energy Journal*, 40.

718 Gianfreda, A., Parisio, L., Pelagatti, M., et al. (2016). The impact of RES in the Italian day-ahead
719 and balancing markets. *Energy Journal*, 37:161–184.

720 Gianfreda, A., Ravazzolo, F., and Rossini, L. (2020). Comparing the forecasting performances
721 of linear models for electricity prices with high res penetration. *International Journal of
722 Forecasting*, 36(3):974–986.

- 723 Gianfreda, A. and Scandolo, G. (2018). *Measuring Model Risk in the European Energy Exchange*,
724 chapter 5, pages 89–110. Springer International Publishing AG.
- 725 Gneiting, T. and Ranjan, R. (2011). Comparing density forecasts using threshold and quantile
726 weighted scoring rules. *Journal of Business and Economic Statistics*, 29:411–422.
- 727 Goldfarb, D. (1970). A family of variable-metric methods derived by variational means.
728 *Mathematics of computation*, 24(109):23–26.
- 729 Gonçalves, C., Pinson, P., and Bessa, R. J. (2021). Towards data markets in renewable energy
730 forecasting. *IEEE Transactions on Sustainable Energy*, 12(1):533–542.
- 731 Groen, J. J. J., Paap, R., and Ravazzolo, F. (2013). Real-time inflation forecasting in a changing
732 world. *Journal of Business & Economic Statistics*, 31:29–44.
- 733 Haldrup, N. and Nielsen, M. Ø. (2006). A regime switching long memory model for electricity
734 prices. *Journal of Econometrics*, 135(1–2):349–376.
- 735 Hansen, P. R., Lunde, A., and Nason, J. M. (2011). The model confidence set. *Econometrica*,
736 79(2):453–497.
- 737 Hickey, E., Loomis, D. G., and Mohammadi, H. (2012). Forecasting hourly electricity prices using
738 ARMAX–GARCH models: An application to MISO hubs. *Energy Economics*, 34(1):307 – 315.
- 739 Hong, T., Pinson, P., and Fan, S. (2014). Global Energy Forecasting Competition 2012.
740 *International Journal of Forecasting*, 30(2):357–363.
- 741 Hong, T., Pinson, P., Wang, Y., Weron, R., Yang, D., and Zareipour, H. (2020). Energy forecasting:
742 A review and outlook. *IEEE Open Access Journal of Power and Energy*, 7:376–388.
- 743 Huurman, C., Ravazzolo, F., and Zhou, C. (2012). The power of weather. *Computational Statistics*
744 *& Data Analysis*, 56(11):3793–3807.
- 745 Jarque, C. M. and Bera, A. K. (1987). A test for normality of observations and regression residuals.
746 *International Statistical Review/Revue Internationale de Statistique*, pages 163–172.
- 747 Jeon, J. and Taylor, J. W. (2016). Short-term density forecasting of wave energy using arma–garch
748 models and kernel density estimation. *International Journal of Forecasting*, 32(3):991 – 1004.

- 749 Johnson, S. G. (2021). The nlopt nonlinear-optimization package. techreport,
750 <http://github.com/stevengj/nlopt>.
- 751 Karakatsani, N. and Bunn, D. (2008). Forecasting electricity prices: the impact of fundamentals
752 and time-varying coefficients. *International Journal of Forecasting*, 24(4):764–785.
- 753 Karakatsani, N. and Bunn, D. W. (2010). Fundamental and behavioural drivers of electricity price
754 volatility. *Studies in Nonlinear Dynamics & Econometrics*, 14(4):1–42.
- 755 Kath, C., Nitka, W., Serafin, T., Weron, T., Zaleski, P., and Weron, R. (2020). Balancing
756 generation from renewable energy sources: Profitability of an energy trader. *Energies*, 13(1).
- 757 Ketterer, J. C. (2014). The impact of wind power generation on the electricity price in Germany.
758 *Energy Economics*, 44:270–280.
- 759 Kezunovic, M., Pinson, P., Obradovic, Z., Grijalva, S., Hong, T., and Bessa, R. (2020). Big data
760 analytics for future electricity grids. *Electric Power Systems Research*, 189:106788.
- 761 Knittel, C. R. and Roberts, M. R. (2005). An empirical examination of restructured electricity
762 prices. *Energy Economics*, 27(5):791–817.
- 763 Koopman, S. J., Ooms, M., and Carnero, M. A. (2007). Periodic seasonal reg-ARFIMA-
764 GARCH models for daily electricity spot prices. *Journal of the American Statistical Association*,
765 102(477):16–27.
- 766 Kwiatkowski, D., Phillips, P. C., Schmidt, P., and Shin, Y. (1992). Testing the null hypothesis of
767 stationarity against the alternative of a unit root: How sure are we that economic time series
768 have a unit root? *Journal of econometrics*, 54(1-3):159–178.
- 769 Kyritsis, E., Andersson, J., and Serletis, A. (2017). Electricity prices, large-scale renewable
770 integration, and policy implications. *Energy Policy*, 101:550–560.
- 771 Laporta, A. G., Merlo, L., and Petrella, L. (2018). Selection of value at risk models for energy
772 commodities. *Energy Economics*, 74:628–643.
- 773 Lisi, F. and Edoli, E. (2018). Analyzing and forecasting zonal imbalance signs in the italian
774 electricity market. *The Energy Journal*, 39(5).

- 775 Maciejowska, K., Nitka, W., and Weron, T. (2021). Enhancing load, wind and solar generation for
776 day-ahead forecasting of electricity prices. *Energy Economics*, 99(C).
- 777 Maciejowska, K. and Nowotarski, J. (2016). A hybrid model for gefcom2014 probabilistic electricity
778 price forecasting. *International Journal of Forecasting*, 32(3):1051 – 1056.
- 779 Maciejowska, K. and Weron, R. (2016). Short-and mid-term forecasting of baseload electricity
780 prices in the UK: The impact of intra-day price relationships and market fundamentals. *IEEE*
781 *Transactions on power systems*, 31(2):994–1005.
- 782 Messner, J. W. and Pinson, P. (2019). Online adaptive lasso estimation in vector autoregressive
783 models for high dimensional wind power forecasting. *International Journal of Forecasting*,
784 35(4):1485 – 1498.
- 785 Nelson, D. B. (1991). Conditional heteroskedasticity in asset returns: A new approach.
786 *Econometrica: Journal of the Econometric Society*, pages 347–370.
- 787 Nowotarski, J. and Weron, R. (2018). Recent advances in electricity price forecasting: a review of
788 probabilistic forecasting. *Renewable and Sustainable Energy Reviews*, 81:1548–1568.
- 789 Oberndorfer, U. (2009). Energy prices, volatility, and the stock market: Evidence from the
790 Eurozone. *Energy Policy*, 37(12):5787–5795.
- 791 Paraschiv, F., Erni, D., and Pietsch, R. (2014). The impact of renewable energies on EEX day-
792 ahead electricity prices. *Energy Policy*, 73:196–210.
- 793 REN21 (2018). Renewables 2018 - global status report. ISBN 978-3-9818107-6-9.
- 794 Said, S. E. and Dickey, D. A. (1984). Testing for unit roots in autoregressive-moving average
795 models of unknown order. *Biometrika*, 71(3):599–607.
- 796 Shah, I. and Lisi, F. (2019). Forecasting of electricity price through a functional prediction of sale
797 and purchase curves. *Journal of Forecasting*,.
- 798 Shanno, D. F. (1970). Conditioning of quasi-newton methods for function minimization.
799 *Mathematics of computation*, 24(111):647–656.

- 800 Terna (2018). Statistical data on electricity in Italy. techreport, <https://www.terna.it/en/electric->
801 [system/statistical-data-forecast/statistical-publications](https://www.terna.it/en/electric-system/statistical-data-forecast/statistical-publications).
- 802 Tibshirani, R. (1996). Regression shrinkage and selection via the lasso. *Journal of the Royal*
803 *Statistical Society: Series B (Methodological)*, 58(1):267–288.
- 804 Uniejewski, B., Marcjasz, G., and Weron, R. (2019). Understanding intraday electricity markets:
805 Variable selection and very short-term price forecasting using lasso. *International Journal of*
806 *Forecasting*, 35(4):1533 – 1547.
- 807 Weron, R. (2007). *Modeling and forecasting electricity loads and prices: A statistical approach*,
808 volume 403. John Wiley & Sons.
- 809 Weron, R. (2014). Electricity price forecasting: a review of the state-of-the-art with a look into
810 the future. *International journal of forecasting*, 30(4):1030–1081.
- 811 Weron, R. and Misoierek, A. (2008). Forecasting spot electricity prices: a comparison of parametric
812 and semiparametric time series models. *International Journal of Forecasting*, 24(4):744–763.
- 813 West, K. D. (1996). Asymptotic inference about predictive ability. *Econometrica: Journal of the*
814 *Econometric Society*, pages 1067–1084.
- 815 Zakoian, J.-M. (1994). Threshold heteroskedastic models. *Journal of Economic Dynamics and*
816 *control*, 18(5):931–955.
- 817 Ziel, F. (2016). Forecasting electricity spot prices using lasso: On capturing the autoregressive
818 intraday structure. *IEEE Transactions on Power Systems*, 31(6):4977–4987.
- 819 Ziel, F., Steinert, R., and Husmann, S. (2015). Efficient modeling and forecasting of electricity
820 spot prices. *Energy Economics*, 47(C):98–111.
- 821 Ziel, F. and Weron, R. (2018). Day-ahead electricity price forecasting with high-dimensional
822 structures: univariate vs. multivariate modeling frameworks. *Energy Economics*, 70:396–420.

823 **Appendix A. GARCH Models**

824 The SGARCH(1,1) is defined as

$$\sigma_t^2 = \omega + \alpha \varepsilon_{t-1}^2 + \beta \sigma_{t-1}^2, \quad (\text{A.1})$$

825 while the EGARCH(1,1) is defined as

$$\log \sigma_t^2 = \omega + \tau g(Z_{t-1}) + \beta \log \sigma_{t-1}^2, \quad (\text{A.2})$$

826 where $g(Z_{t-1}) = \kappa Z_{t-1} + \eta(|Z_{t-1}| - \mathbb{E}(Z_{t-1}))$, and it allows the conditional variance process to respond
827 asymmetrically.

828 To account for asymmetries in volatility, making it a function of positive and negative values of the
829 innovations, we consider the TGARCH(1,1) process (Zakoian, 1994), defined as follows

$$\sigma_t = \omega + \alpha_1^+ \varepsilon_{t-1}^+ + \alpha_1^- \varepsilon_{t-1}^- + \beta \sigma_{t-1} \quad (\text{A.3})$$

830 where $\varepsilon_{t-1}^+ = \varepsilon_{t-1}$ if $\varepsilon_{t-1} > 0$ and 0 otherwise, $\varepsilon_{t-1}^- = \varepsilon_{t-1}$ if $\varepsilon_{t-1} \leq 0$ and 0 otherwise.

831 Finally, the adopted GARCH(1,1)-in-mean (or simply, GARCH-M) is defined as

$$y_t = \mu + c\sigma_t + \varepsilon_t \text{ with } \sigma_t^2 = \omega + \alpha \varepsilon_{t-1}^2 + \beta \sigma_{t-1}^2. \quad (\text{A.4})$$

832 **Appendix B. Tables**

Years	Gas	Oil	Coal	Other	Hydro	Wind	Solar	Geothermal	Biomass	Waste
<i>North</i>										
2015	0.608	0.000	0.000	0.665	0.807	0.012	0.371		0.359	0.867
2016	0.568	0.000	0.000	0.710	0.811	0.004	0.357		0.373	0.879
2017	0.625	0.000	0.220	0.716	0.816	0.004	0.357		0.327	0.941
2018	0.626	0.091	0.336	0.760	0.799	0.003	0.358		0.343	0.962
2019	0.608	0.054	0.172	0.713	0.818	0.004	0.370		0.316	0.792
<i>Central North</i>										
2015	0.130	0.000	0.003	0.020	0.056	0.014	0.118	1.000	0.090	
2016	0.137	0.002	0.001	0.020	0.068	0.013	0.114	1.000	0.067	
2017	0.126	0.003	0.001	0.036	0.062	0.014	0.124	1.000	0.027	
2018	0.109	0.004	0.000	0.032	0.066	0.014	0.123	1.000	0.022	
2019	0.075	0.005	0.000	0.051	0.054	0.016	0.124	1.000	0.042	
<i>Central South</i>										
2015	0.085	0.001	0.752	0.142	0.081	0.175	0.153		0.039	0.101
2016	0.140	0.001	0.635	0.134	0.073	0.188	0.169		0.011	0.087
2017	0.138	0.002	0.476	0.116	0.072	0.182	0.168		0.019	0.000
2018	0.160	0.001	0.396	0.066	0.082	0.172	0.183		0.031	0.000
2019	0.123	0.001	0.200	0.104	0.071	0.178	0.173		0.119	0.000
<i>South</i>										
2015	0.000	0.000	0.000	0.047	0.044	0.504	0.234		0.329	0.032
2016	0.000	0.000	0.000	0.048	0.039	0.497	0.234		0.371	0.034
2017	0.001	0.000	0.000	0.049	0.038	0.536	0.232		0.470	0.059
2018	0.003	0.000	0.000	0.049	0.040	0.522	0.226		0.477	0.038
2019	0.129	0.000	0.189	0.089	0.039	0.531	0.224		0.420	0.208
<i>Sicily</i>										
2015	0.177	0.971	0.039	0.040	0.006	0.185	0.082		0.054	
2016	0.155	0.997	0.157	0.013	0.003	0.188	0.083		0.053	
2017	0.111	0.994	0.085	0.014	0.003	0.166	0.080		0.042	
2018	0.102	0.717	0.075	0.014	0.002	0.190	0.076		0.037	
2019	0.065	0.763	0.065	0.029	0.009	0.168	0.077		0.023	
<i>Sardinia</i>										
2015	0.000	0.028	0.205	0.086	0.006	0.110	0.042		0.130	
2016	0.000	0.001	0.207	0.076	0.006	0.111	0.042		0.126	
2017	0.000	0.002	0.218	0.070	0.009	0.099	0.039		0.114	
2018	0.000	0.187	0.193	0.079	0.011	0.100	0.033		0.089	
2019	0.000	0.176	0.374	0.014	0.009	0.103	0.033		0.081	

Table B.7: Generation Shares across Zones and Years, as proportion of total national yearly production by source according to the classification for technologies adopted by ENTSO-E. Note that Italy does not generate electricity using nuclear, marine, peat and shale oil. Data: ENTSO-E from 2015-2019.

	2015	2016	2017	2018	2019	2015	2016	2017	2018	2019	2015	2016	2017	2018	2019	2015	2016	2017	2018	2019
	Italy					France					Austria					Slovenia				
Nuclear						0.522	0.569	0.512	0.478	0.483						0.176	0.190	0.187	0.186	0.186
Gas	0.203	0.306	0.426	0.417	0.491	0.051	0.055	0.054	0.090	0.091	0.217	0.215	0.207	0.203	0.210	0.124	0.134	0.132	0.131	0.131
Coal	0.017	0.073	0.094	0.086	0.071	0.040	0.026	0.024	0.030	0.030	0.057	0.037	0.028	0.027	0.028	0.310	0.251	0.248	0.247	0.247
Oil	0.049	0.090	0.053	0.026	0.015	0.055	0.060	0.043	0.047	0.025	0.009	0.009	0.008	0.008	0.008	0.000	0.000	0.016	0.016	0.016
Other	0.369	0.142	0.018	0.062	0.011	0.001	0.001	0.001	0.001	0.001	0.001	0.001	0.001	0.001	0.001					
Marine						0.002	0.002	0.002	0.002	0.002										
Hydro	0.213	0.223	0.234	0.235	0.234	0.194	0.212	0.191	0.188	0.186	0.555	0.553	0.553	0.545	0.522	0.311	0.337	0.331	0.330	0.330
Wind	0.082	0.089	0.096	0.099	0.102	0.085	0.013	0.110	0.095	0.104	0.102	0.120	0.125	0.131	0.142	0.001	0.001	0.001	0.001	0.001
Solar	0.049	0.049	0.050	0.050	0.050	0.051	0.061	0.062	0.054	0.063	0.028	0.035	0.048	0.054	0.056	0.066	0.072	0.071	0.074	0.074
Geother	0.008	0.009	0.009	0.009	0.009						0.000	0.000	0.000	0.000	0.000					
Biomass	0.009	0.016	0.017	0.014	0.016	0.000	0.002	0.001	0.014	0.015	0.022	0.023	0.022	0.022	0.023	0.004	0.005	0.005	0.005	0.005
Waste	0.001	0.003	0.003	0.002	0.001						0.007	0.007	0.007	0.007	0.007	0.009	0.011	0.011	0.011	0.011
other RES	0.000	0.000	0.000	0.000	0.000						0.001	0.002	0.002	0.002	0.002	0.000	0.000	0.000	0.000	0.000
	Switzerland																			
Nuclear	0.274	0.269	0.230	0.212	0.210															
Hydro	0.726	0.731	0.770	0.788	0.790															

Table B.8: Technology Shares over Total Installed Capacity. Data: ENTSO-E.

	1	2	3	4	5	6	7	8	9
EX ₄ X	4.790	4.964	5.082	5.138	4.876	6.236	8.137	9.412	9.782
EX ₄ X-F	4.170 ***	4.345 **	4.629 *	4.644 *	4.640	5.498 ***	5.482 ***	6.042 ***	6.562 ***
EX ₄ X-LF	4.170 ***	4.343 **	4.624 *	4.652 *	4.646	5.496 ***	5.480 ***	6.042 ***	6.553 ***
EX ₄ X-SGARCHX	4.811	4.984	5.090	5.153	4.961	6.235	8.159	9.382	9.939
EX ₄ X-SGARCHX-F	4.170 ***	4.351 ***	4.592 **	4.558 **	4.597	5.452 ***	5.438 ***	6.099 ***	6.573 ***
EX ₄ X-SGARCHX-LF	4.172 ***	4.342 ***	4.580 **	4.536 **	4.585	5.459 ***	5.434 ***	6.068 ***	6.593 ***
	10	11	12	13	14	15	16	17	18
EX ₄ X	8.341	7.515	6.409	6.888	8.459	8.565	8.546	7.628	7.391
EX ₄ X-F	6.442 ***	6.325 ***	5.433 ***	5.681 ***	6.728 ***	6.531 ***	6.330 ***	5.263 ***	5.205 ***
EX ₄ X-LF	6.437 ***	6.329 ***	5.445 ***	5.694 ***	6.738 ***	6.529 ***	6.344 ***	5.271 ***	5.207 ***
EX ₄ X-SGARCHX	8.501	7.663	6.612	7.074	8.626	9.006	9.116	8.105	7.558
EX ₄ X-SGARCHX-F	6.481 ***	6.273 ***	5.368 ***	5.525 ***	6.632 ***	6.550 ***	6.469 ***	5.356 ***	5.242 ***
EX ₄ X-SGARCHX-LF	6.460 ***	6.307 ***	5.353 ***	5.597 ***	6.635 ***	6.551 ***	6.453 ***	5.351 ***	5.278 ***
	19	20	21	22	23	24	<i>Avg</i> ₁₋₂₄	<i>Avg</i> ₈₋₂₀	
EX ₄ X	6.719	5.934	5.105	4.457	3.732	4.423	6.605	7.814	
EX ₄ X-F	5.354 ***	5.295 ***	4.668 **	4.033 ***	3.142 ***	3.892 ***	5.264	5.938	
EX ₄ X-LF	5.357 ***	5.282 ***	4.673 **	4.036 ***	3.149 ***	3.895 ***	5.266	5.941	
EX ₄ X-SGARCHX	6.739	6.080	5.269	4.487	3.749	4.580	6.745	8.031	
EX ₄ X-SGARCHX-F	5.400 ***	5.152 ***	4.645 **	4.030 ***	3.161 ***	5.137	5.302	5.932	
EX ₄ X-SGARCHX-LF	5.362 ***	5.178 ***	4.647 **	4.032 ***	3.158 ***	5.137	5.303	5.937	

Table B.9: RMSEs of the best performing model with ENTSO-E forecasts (EX₄X and EX₄X-SGARCHX) and with ETR forecasts for *fast* (EX₄X-F and EX₄X-SGARCHX-F) and *less fast* (EX₄X-LF and EX₄X-SGARCHX-LF) models, over 365 forecasts computed for the whole 2019. The average over the 24 hours and the average over peak hours 8-20 are also included. Grey cells refer to specifications excluded from the Superior Set of Models selected according to the Hansen-Luden-Nason MCS procedure at $\alpha = 0.15$. ***, ** and * indicate that a model is more accurate than the EX₄X benchmark model at the 0.1%, 1%, 5% significance levels according to the one-sided DM test. Absence of stars indicates that none of the alternative specifications provides more accurate forecasts.

	1	2	3	4	5	6	7	8	9
EX ₄ X	0.261	0.247	0.239	0.232	0.232	0.240	0.263	0.290	0.310
EX ₄ X-F	0.285***	0.284	0.269	0.246	0.241	0.232*	0.250***	0.282***	0.297***
EX ₄ X-LF	0.284***	0.284	0.269	0.246	0.241	0.232 •	0.249***	0.282***	0.297***
EX ₄ X-SGARCHX	0.109***	0.104***	0.103***	0.099***	0.098***	0.098***	0.111***	0.142***	0.179***
EX ₄ X-SGARCHX-F	0.113***	0.120***	0.098***	0.078***	0.078***	0.077***	0.089***	0.094***	0.128***
EX ₄ X-SGARCHX-LF	0.110***	0.125***	0.099***	0.078***	0.079***	0.075***	0.085***	0.095***	0.126***
	10	11	12	13	14	15	16	17	18
EX ₄ X	0.306	0.301	0.298	0.280	0.284	0.296	0.300	0.300	0.291
EX ₄ X-F	0.296***	0.295***	0.301***	0.307***	0.286***	0.279***	0.300***	0.307***	0.319***
EX ₄ X-LF	0.296***	0.295***	0.302***	0.307***	0.287***	0.279***	0.300***	0.307***	0.319***
EX ₄ X-SGARCHX	0.173***	0.164***	0.164***	0.140***	0.153***	0.173***	0.175***	0.166***	0.146***
EX ₄ X-SGARCHX-F	0.125***	0.113***	0.121***	0.117***	0.108***	0.118***	0.125***	0.129***	0.171***
EX ₄ X-SGARCHX-LF	0.126***	0.112***	0.119***	0.117***	0.106***	0.118***	0.125***	0.132***	0.169***
	19	20	21	22	23	24	Avg_1-24	Avg_8-20	
EX ₄ X	0.293	0.296	0.295	0.285	0.273	0.248	0.278	0.296	
EX ₄ X-F	0.313***	0.309***	0.301***	0.296***	0.289***	0.245***	0.285	0.299	
EX ₄ X-LF	0.313***	0.309***	0.301***	0.296***	0.289***	0.245***	0.285	0.299	
EX ₄ X-SGARCHX	0.144***	0.143***	0.134***	0.116***	0.107***	0.107***	0.137	0.159	
EX ₄ X-SGARCHX-F	0.141***	0.131***	0.121***	0.110***	0.105***	0.084***	0.112	0.125	
EX ₄ X-SGARCHX-LF	0.144***	0.131***	0.122***	0.109***	0.107***	0.084***	0.112	0.125	

Table B.10: CRPSs of the best performing model with ENTSO-E forecasts (EX₄X and EX₄X-SGARCHX) and with ETR forecasts for *fast* (EX₄X-F and EX₄X-SGARCHX-F) and *less fast* (EX₄X-LF and EX₄X-SGARCHX-LF) models, over 365 forecasts computed for the whole 2019. The average over the 24 hours and the average over peak hours 8-20 are also included. Grey cells refer to specifications excluded from the Superior Set of Models selected according to the Hansen-Luden-Nason MCS procedure at $\alpha = 0.15$. ***, **, * and • indicate that a model is more accurate than the EX₄X benchmark model at the 0.1%, 1%, 5% and 10% significance levels according to the one-sided DM test. Absence of stars/bullets indicates that none of the alternative specifications provides more accurate forecasts.

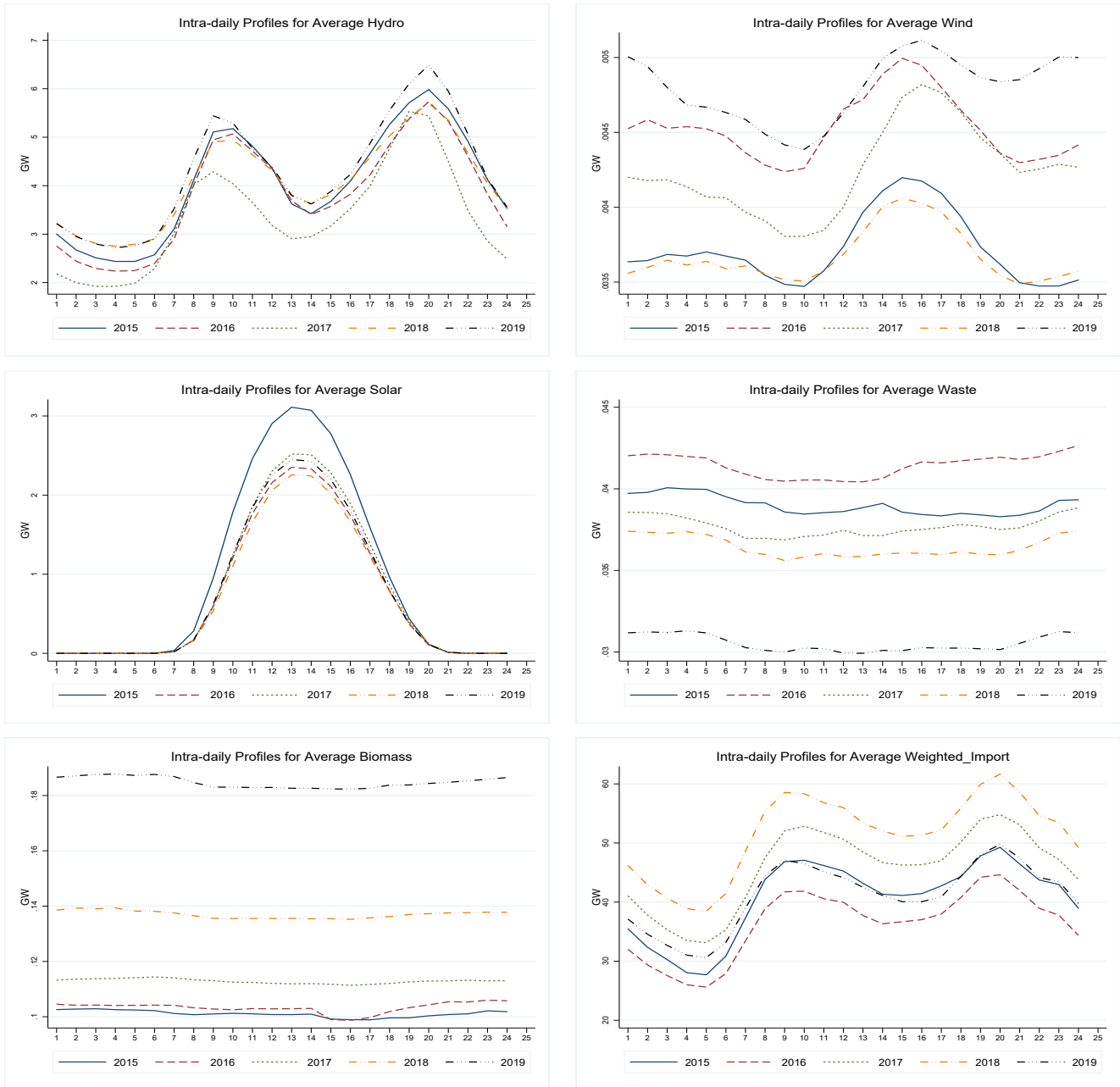


Figure C.3: Intra-daily Profiles of some Exogenous Regressors from 2015 to 2019. Data: ENTSO-E.

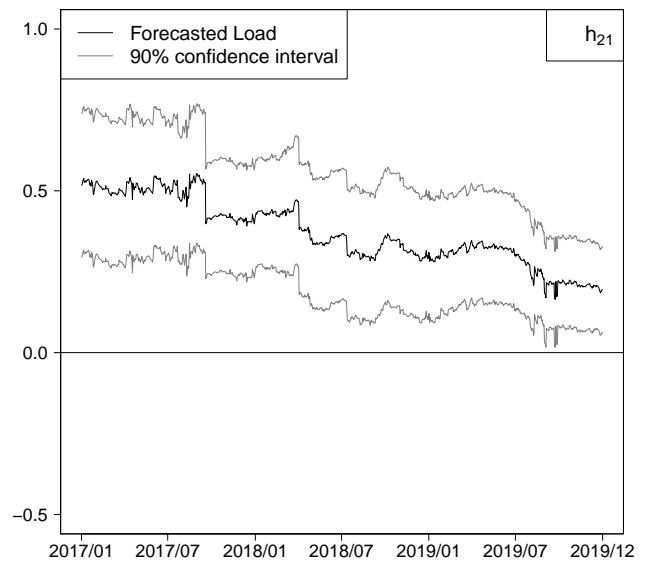
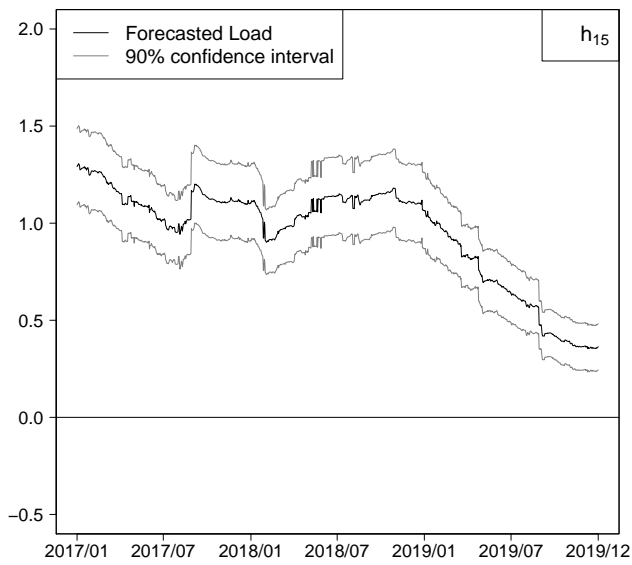
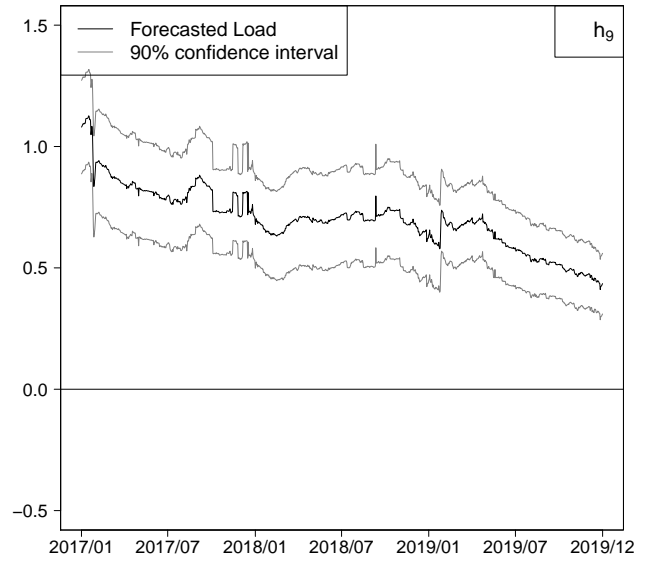
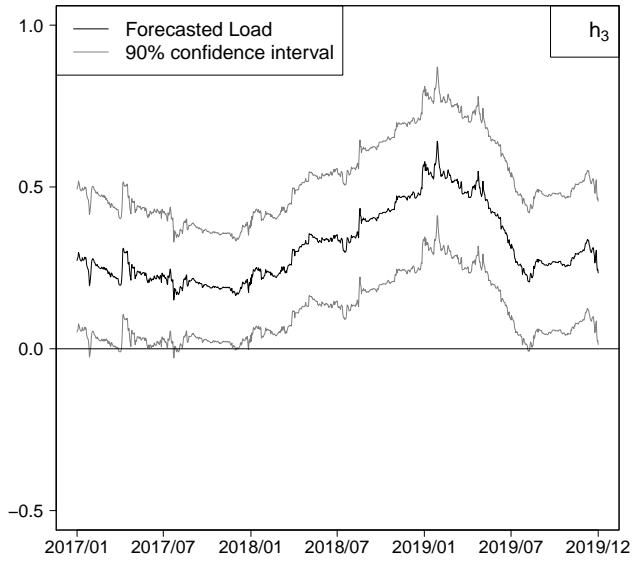


Figure C.4: Estimated coefficients for ENTSO-E Forecasted Load by using the EX_4X model at hours 3, 9, 15, and 21. Robust Confidence Intervals at 90% are also reported over the out-of-sample period from 2017/01/01 to 2019/12/31.

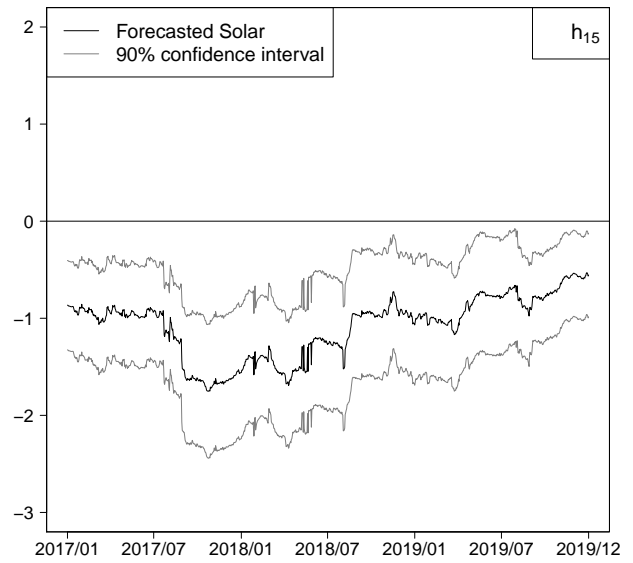
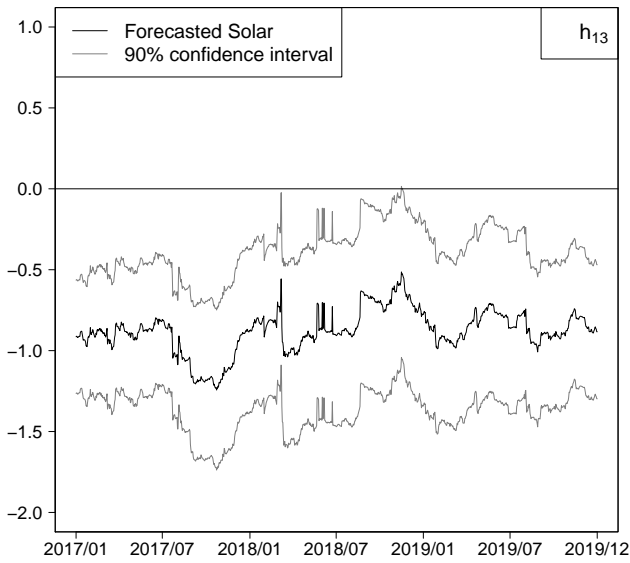
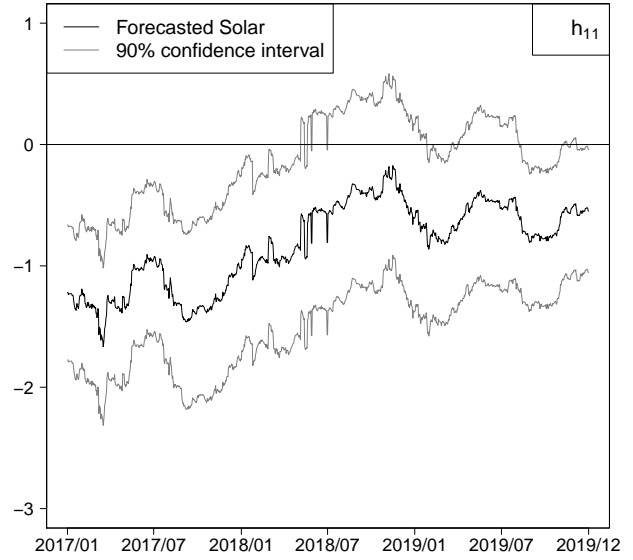
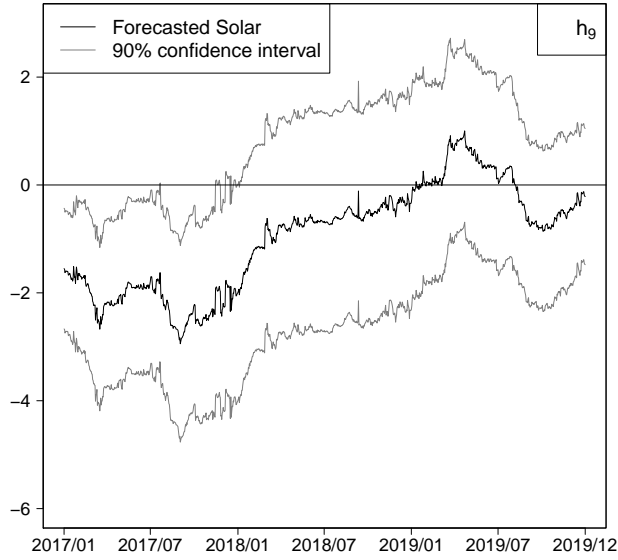


Figure C.5: Estimated coefficients for ENTSO-E Forecasted Solar PV Power using the EX_4X model at hours 9, 11, 13 and 15. Robust Confidence Intervals at 90% are also reported over the out-of-sample period from 2017/01/01 to 2019/12/31.

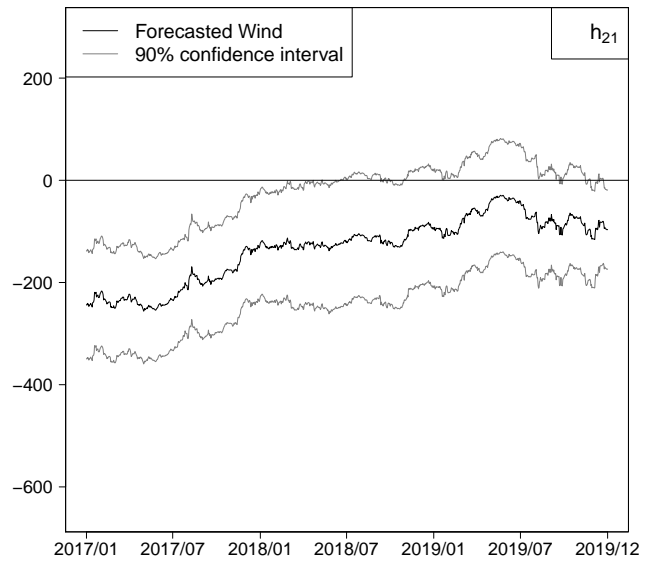
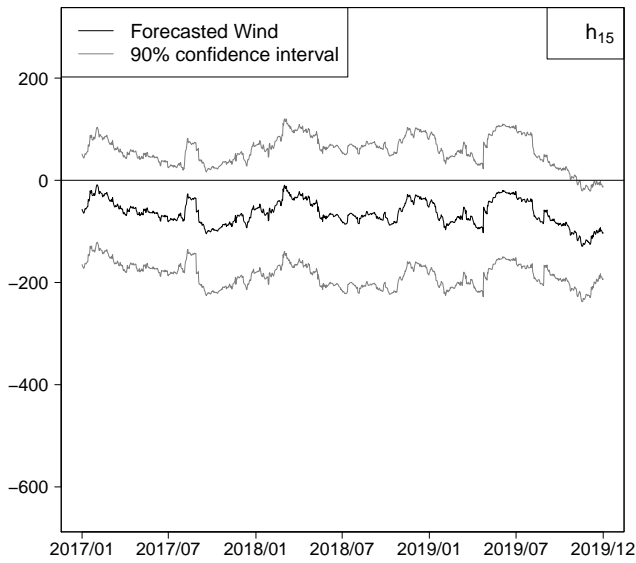
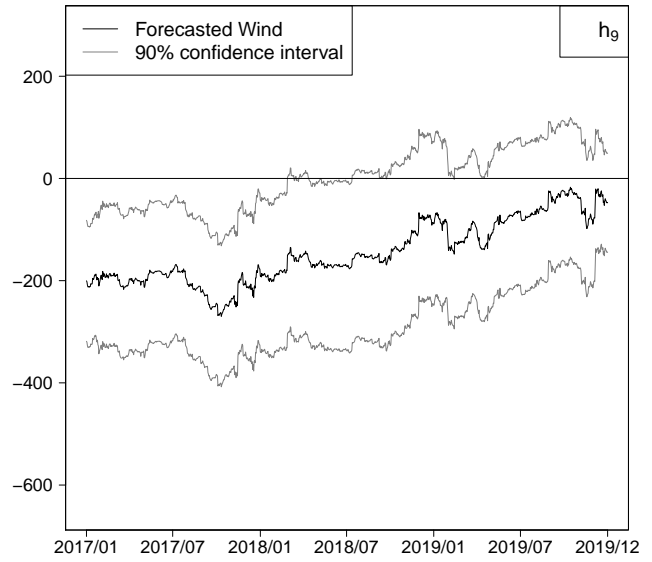
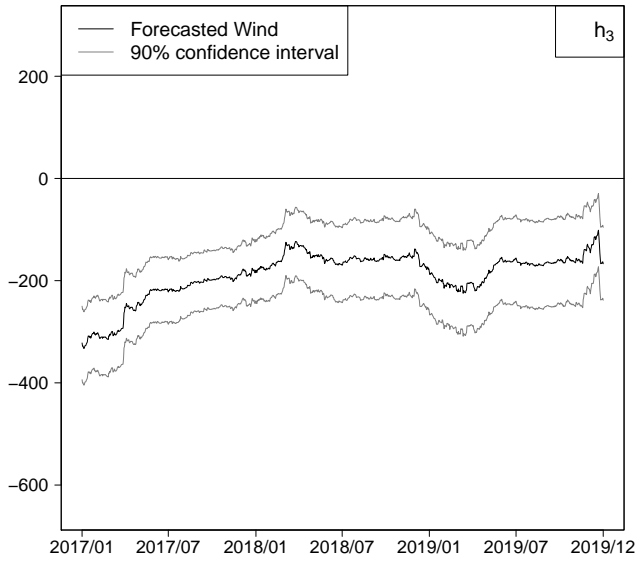


Figure C.6: Estimated coefficients for ENTSO-E Forecasted Wind using the EX_4X model at hours 3, 9, 15, and 21. Robust Confidence Intervals at 90% are also reported over the out-of-sample period from 2017/01/01 to 2019/12/31.

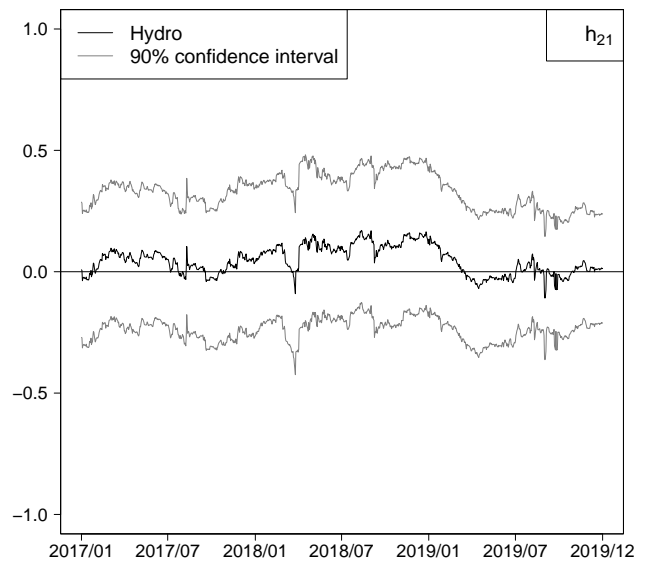
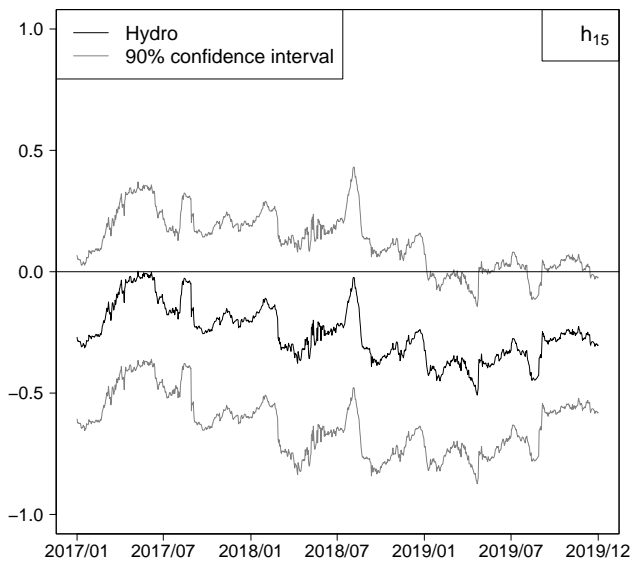
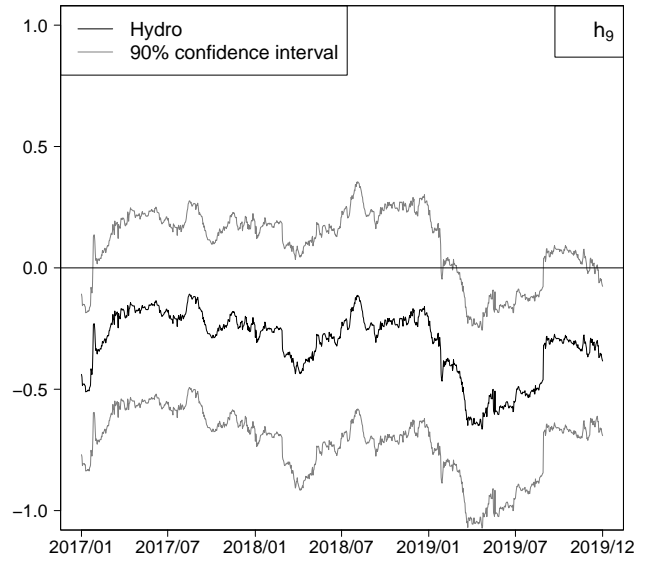
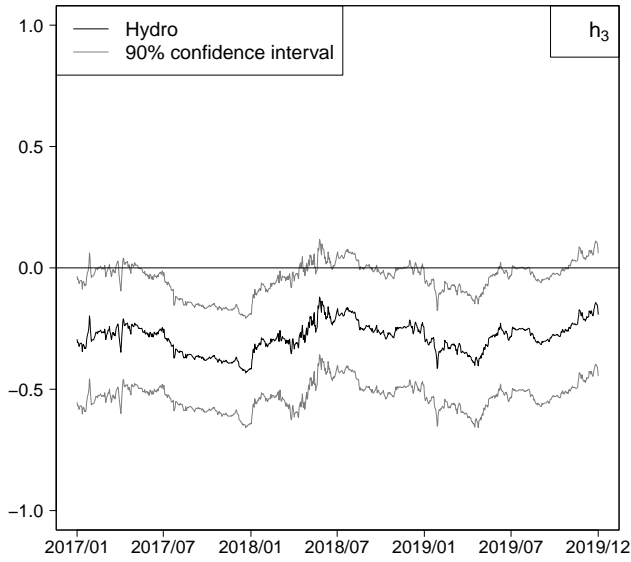


Figure C.7: Estimated coefficients for Hydro using the EX_4X model at hours 3, 9, 15, and 21. Robust Confidence Intervals at 90% are also reported over the out-of-sample period from 2017/01/01 to 2019/12/31.

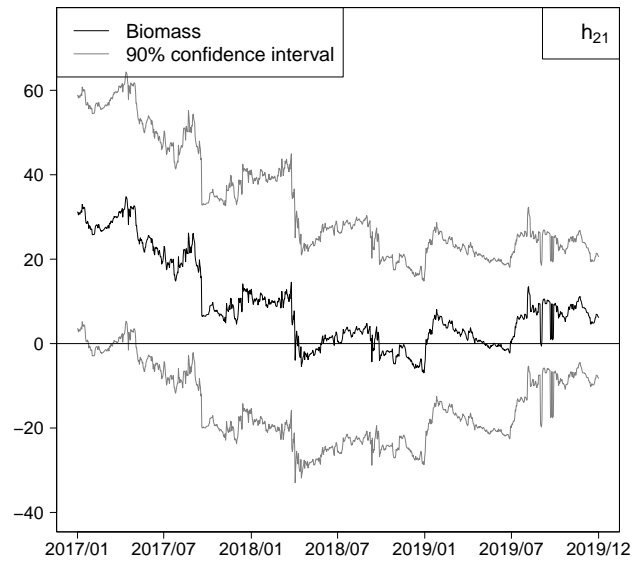
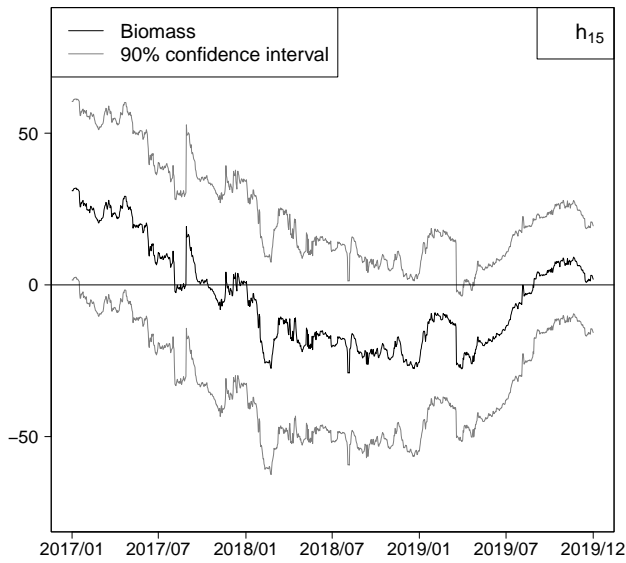
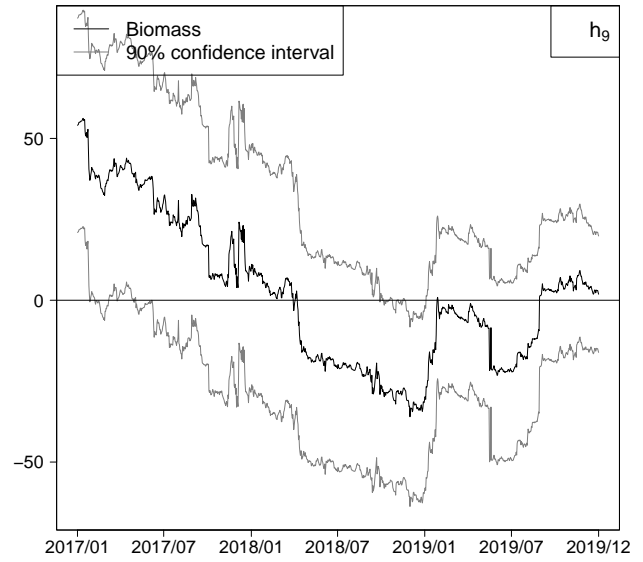
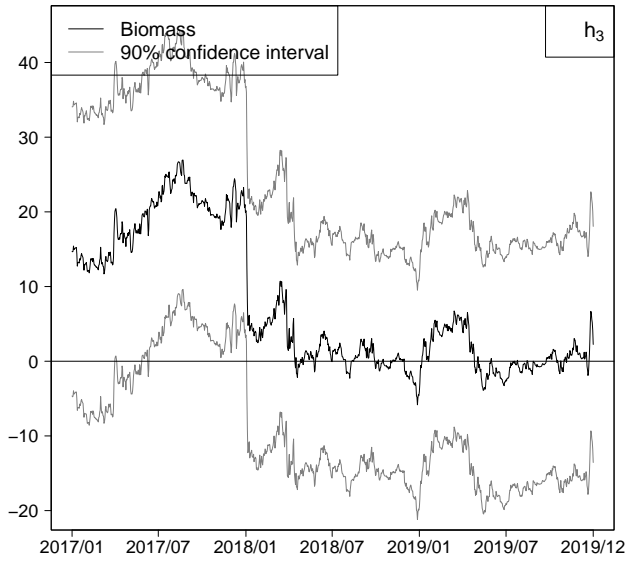


Figure C.8: Estimated coefficients for Biomass using the EX_4X model at hours 3, 9, 15, and 21. Robust Confidence Intervals at 90% are also reported over the out-of-sample period from 2017/01/01 to 2019/12/31.

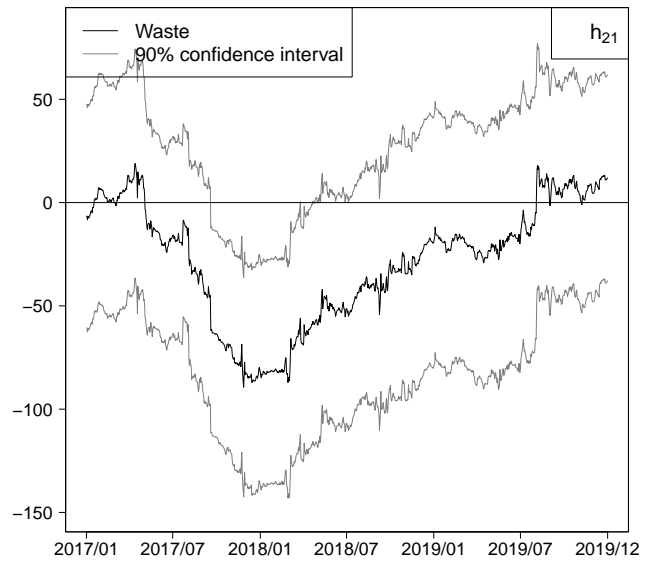
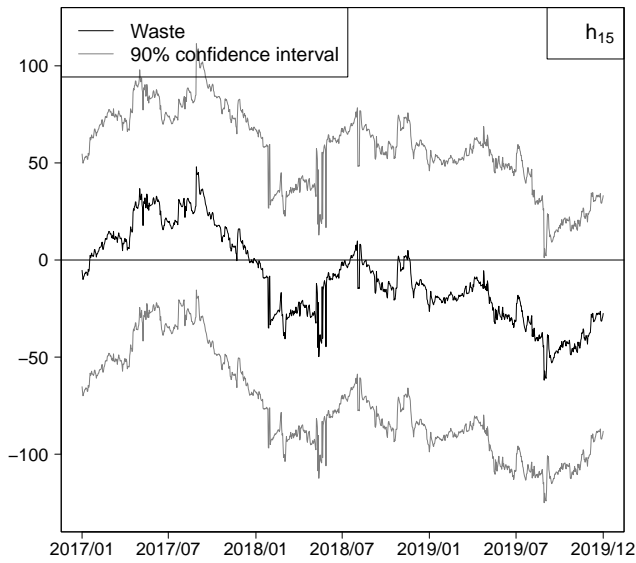
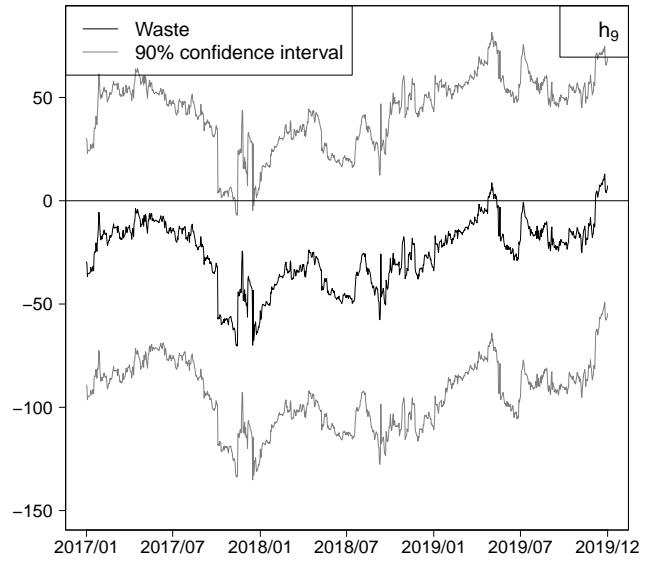
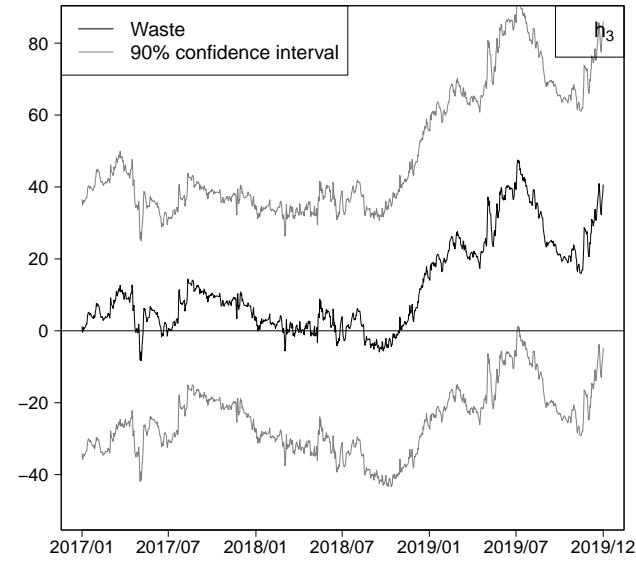


Figure C.9: Estimated coefficients for Waste using the EX_4X model at hours 3, 9, 15, and 21. Robust Confidence Intervals at 90% are also reported over the out-of-sample period from 2017/01/01 to 2019/12/31.

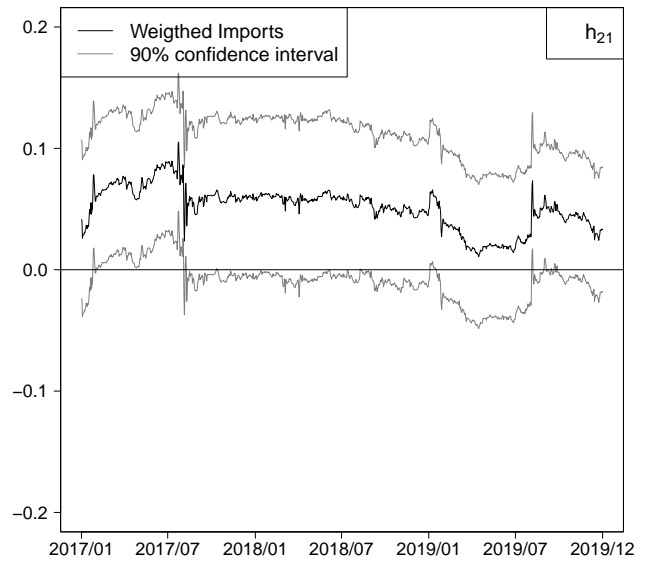
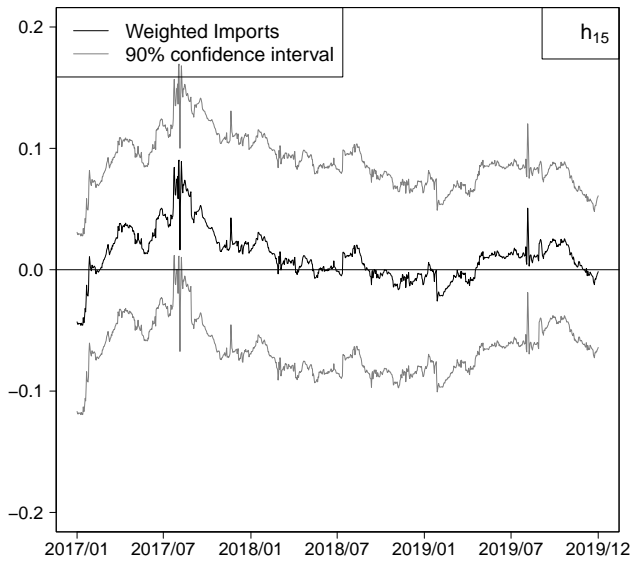
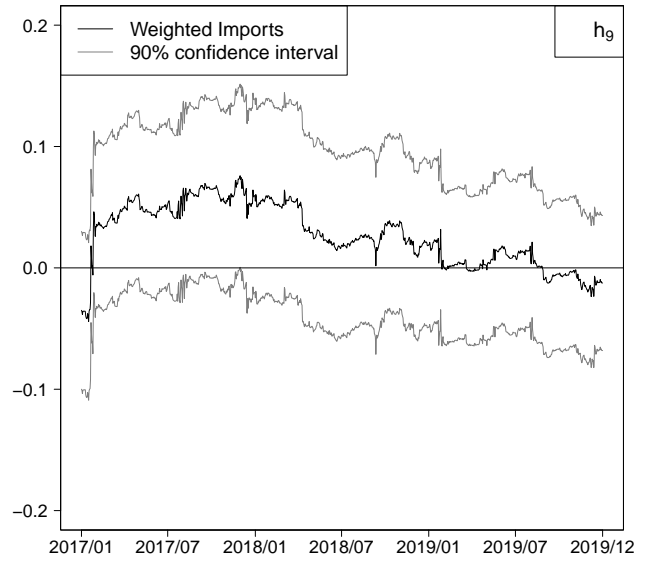
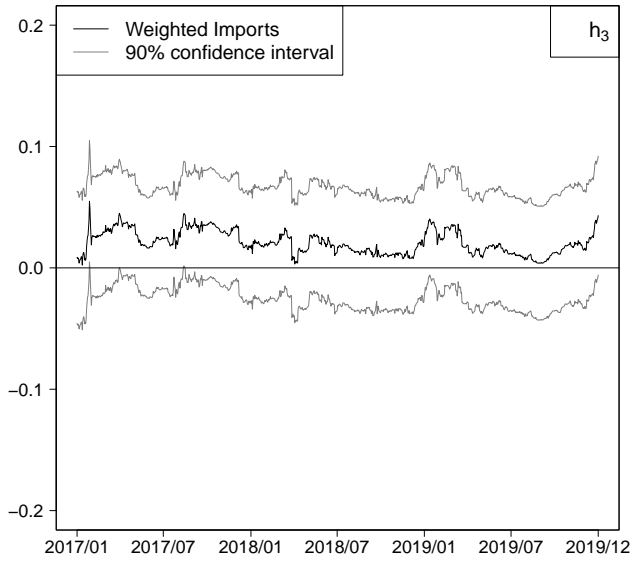


Figure C.10: Estimated coefficients for Weighted Imports using the EX_4X model at hours 3, 9, 15, and 21. Robust Confidence Intervals at 90% are also reported over the out-of-sample period from 2017/01/01 to 2019/12/31.

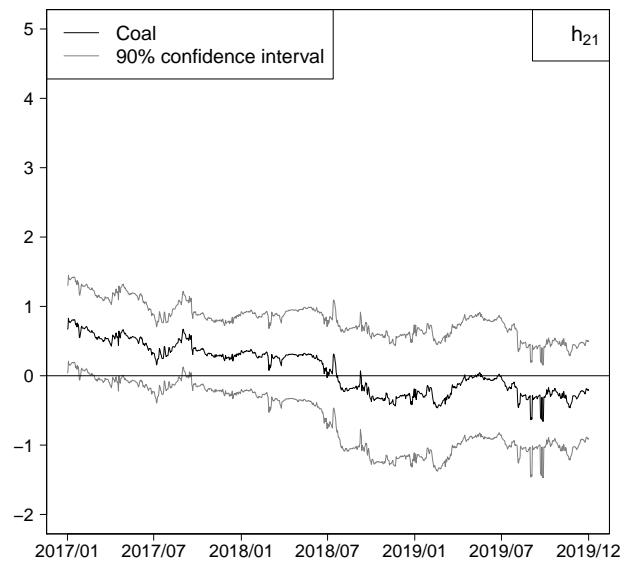
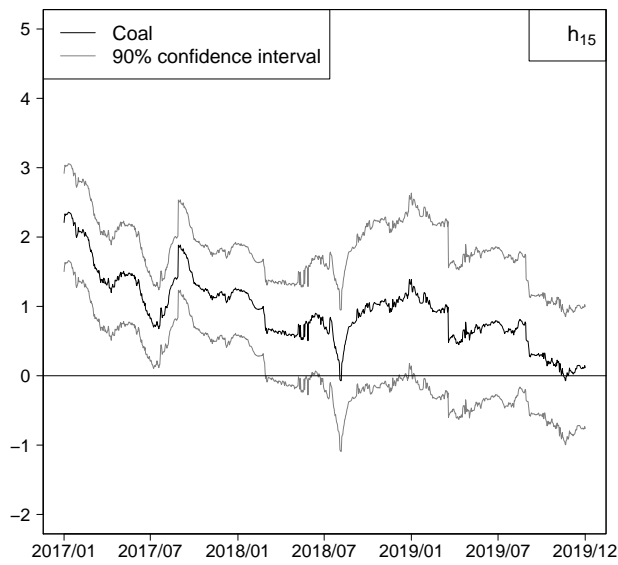
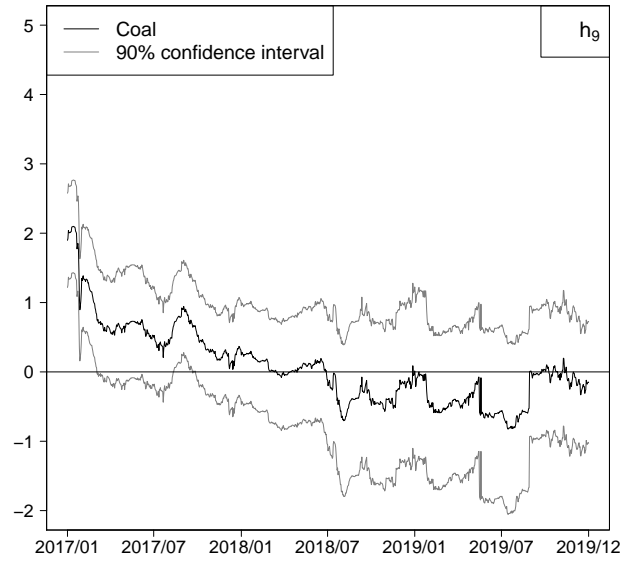
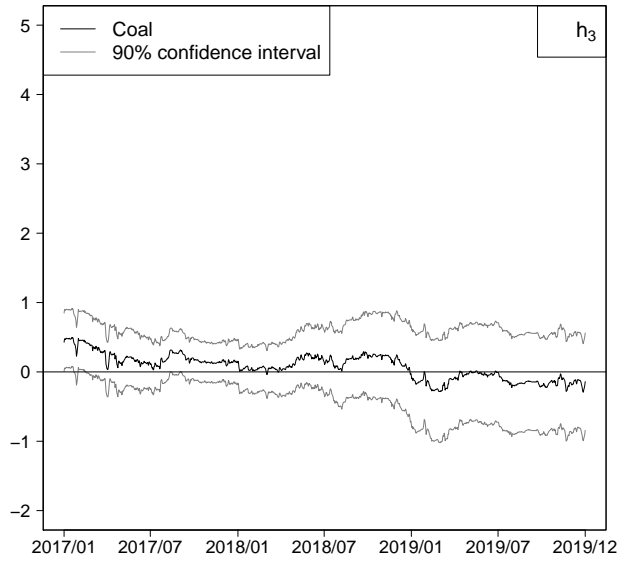


Figure C.11: Estimated coefficients for Coal using the EX_4X model at hours 3, 9, 15, and 21. Robust Confidence Intervals at 90% are also reported over the out-of-sample period from 2017/01/01 to 2019/12/31.

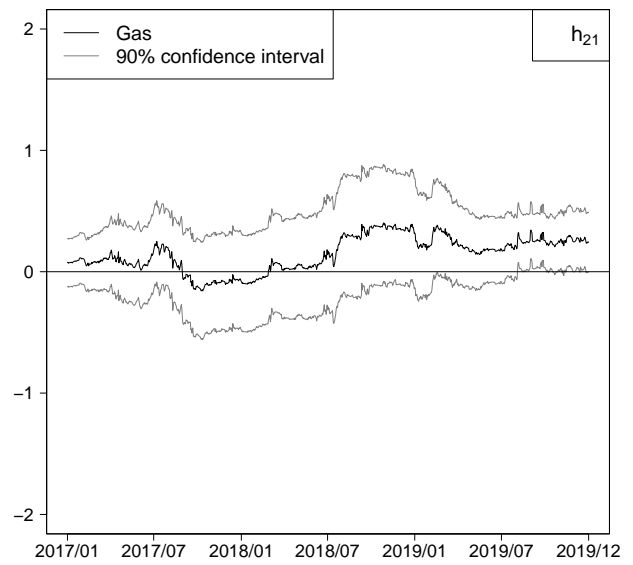
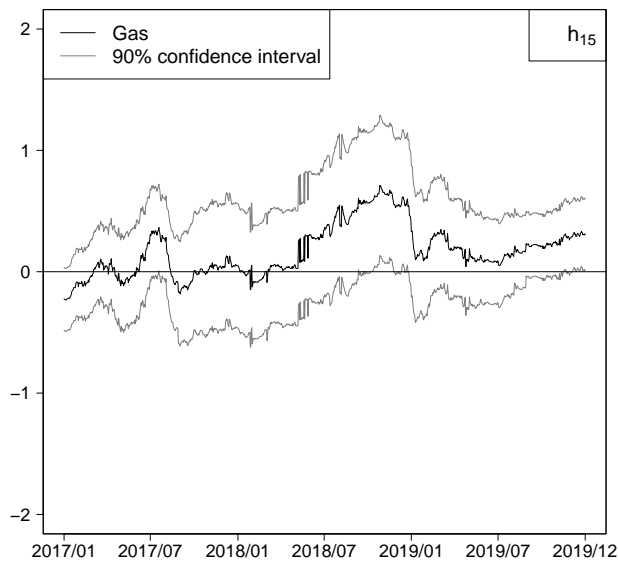
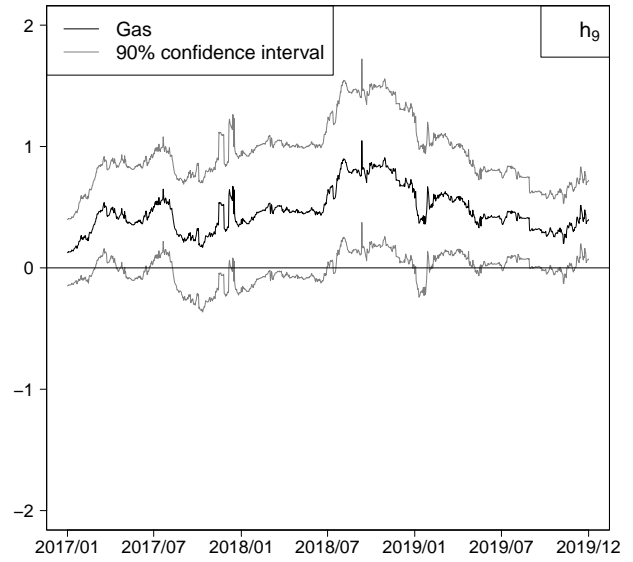
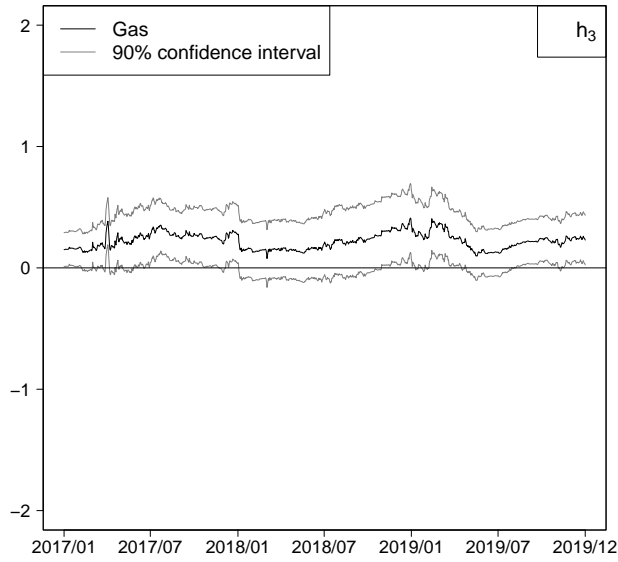


Figure C.12: Estimated coefficients for Natural Gas using the EX_4X model at hours 3, 9, 15, and 21. Robust Confidence Intervals at 90% are also reported over the out-of-sample period from 2017/01/01 to 2019/12/31.

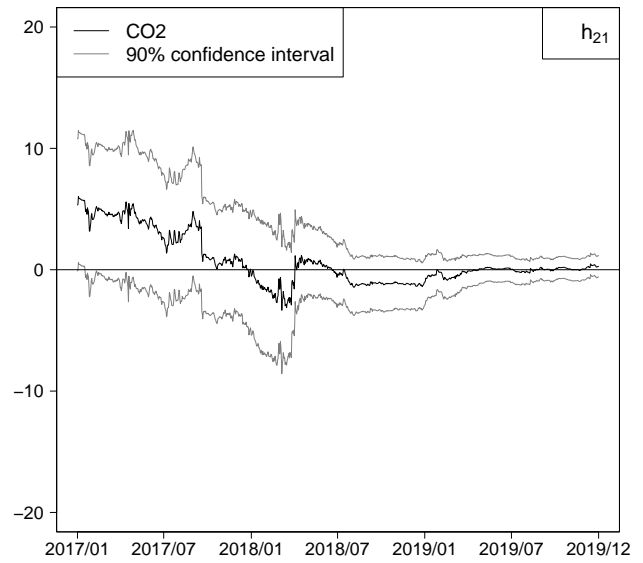
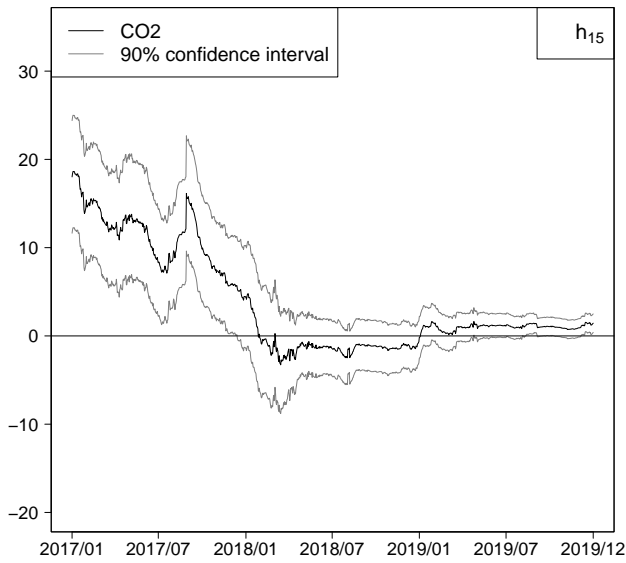
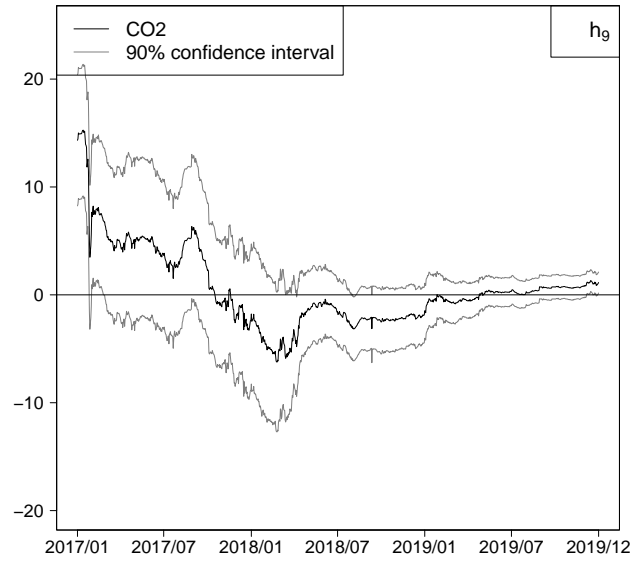
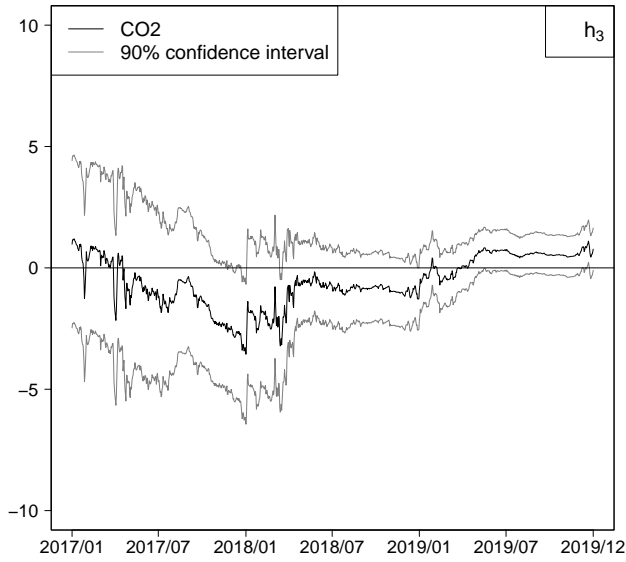


Figure C.13: Estimated coefficients for CO₂ using the EX₄X model at hours 3, 9, 15, and 21. Robust Confidence Intervals at 90% are also reported over the out-of-sample period from 2017/01/01 to 2019/12/31.